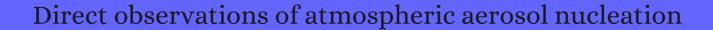
CITATION REPORT List of articles citing



DOI: 10.1126/science.1227385 Science, 2013, 339, 943-6.

Source: https://exaly.com/paper-pdf/55768282/citation-report.pdf

Version: 2024-04-28

This report has been generated based on the citations recorded by exaly.com for the above article. For the latest version of this publication list, visit the link given above.

The third column is the impact factor (IF) of the journal, and the fourth column is the number of citations of the article.

#	Paper	IF	Citations
809	MEASUREMENT AND REPORTING OF RADON EXPOSURES. 2012 , 12, 1-191		11
808	References. 2012 , 12, 169-191		
807	Comparing simulated and experimental molecular cluster distributions. 2013 , 165, 75-89		27
806	Assessment of binding energies of atmospherically relevant clusters. 2013 , 15, 16442-5		103
805	Case studies of new particle formation and evaporation processes in the western Mediterranean regional background. 2013 , 81, 651-659		18
804	Atmospheric nanoparticles and climate change. 2013 , 59, 4006-4019		8
803	Molecular understanding of sulphuric acid-amine particle nucleation in the atmosphere. 2013 , 502, 359-	-63	585
802	Quantitative and time-resolved nanoparticle composition measurements during new particle formation. 2013 , 165, 25-43		27
801	How do organic vapors contribute to new-particle formation?. 2013 , 165, 91-104		84
800	Nucleation events for the formation of charged aerosol particles at a tropical station Preliminary results. 2013 , 132-133, 239-252		25
799	Atmospheric science. The aerosol nucleation puzzle. <i>Science</i> , 2013 , 339, 911-2	33.3	34
79 ⁸	Fundamental and overtone vibrational spectroscopy, enthalpy of hydrogen bond formation and equilibrium constant determination of the methanol-dimethylamine complex. 2013 , 15, 10194-206		65
797	Interaction of glycine with common atmospheric nucleation precursors. 2013 , 117, 12990-7		43
796	Vibrational spectra and fragmentation pathways of size-selected, D2-tagged ammonium/methylammonium bisulfate clusters. 2013 , 117, 13265-74		28
795	Real-time monitoring of emissions from monoethanolamine-based industrial scale carbon capture facilities. 2013 , 47, 14306-14		45
794	Performance of diethylene glycol-based particle counters in the sub-3 nm size range. 2013 , 6, 1793-180-	4	54
793	Characterisation of organic contaminants in the CLOUD chamber at CERN. 2013 ,		1

792	COMPASS ICOMparative Particle formation in the Atmosphere using portable Simulation chamber Study techniques. 2013 , 6, 3407-3423	3
791	Sub 3 nm particle size and composition dependent response of a nano-CPC battery. 2013 ,	
790	Free energy barrier in the growth of sulfuric acid-ammonia and sulfuric acid-dimethylamine clusters. 2013 , 139, 084312	118
789	Molecular understanding of atmospheric particle formation from sulfuric acid and large oxidized organic molecules. 2013 , 110, 17223-8	249
788	Semi-empirical parameterization of size-dependent atmospheric nanoparticle growth in continental environments. 2013 , 13, 7665-7682	21
787	Identification and quantification of particle growth channels during new particle formation. 2013 , 13, 10215-10225	16
786	Estimating the contribution of ionlibn recombination to sub-2 nm cluster concentrations from atmospheric measurements. 2013 , 13, 11391-11401	17
7 ⁸ 5	Long-term observations of cluster ion concentration, sources and sinks in clear sky conditions at the high-altitude site of the Puy de Dîme, France. 2013 , 13, 11573-11594	16
784	Growth of atmospheric nano-particles by heterogeneous nucleation of organic vapor. 2013 , 13, 6523-6531	14
783	Formation and growth of nucleated particles into cloud condensation nuclei: modellheasurement comparison. 2013 , 13, 7645-7663	67
782	Estimating neutral nanoparticle steady-state size distribution and growth according to measurements of intermediate air ions. 2013 , 13, 9597-9603	2
781	Marine nanogels as a source of atmospheric nanoparticles in the high Arctic. 2013 , 40, 3738-3743	48
780	Photooxidation of dimethylsulfide (DMS) in the Canadian Arctic. 2013, 10, 6793-6806	11
779	Terpenoid emissions from fully grown east Siberian <i>Larix cajanderi</i> trees. 2013 , 10, 4705-4719	8
778	Where do herbivore-induced plant volatiles go?. 2013 , 4, 185	89
777	New foliage growth is a significant, unaccounted source for volatiles in boreal evergreen forests. 2014 , 11, 1331-1344	47
776	Sub-3 nm particle size and composition dependent response of a nano-CPC battery. 2014 , 7, 689-700	64
775	Difference in particle formation at a mountaintop location during spring and summer: Implications for the role of sulfuric acid and organics in nucleation. 2014 , 119, 12,246-12,255	14

774	Cloud forming potential of oligomers relevant to secondary organic aerosols. 2014 , 41, 6538-6545	17
773	Atmospheric processes on ice nanoparticles in molecular beams. 2014 , 2, 4	14
772	Comparing three vegetation monoterpene emission models to measured gas concentrations with a model of meteorology, air chemistry and chemical transport. 2014 , 11, 5425-5443	23
771	Trimethylamine emissions in animal husbandry. 2014 , 11, 5073-5085	34
770	Rapid autoxidation forms highly oxidized RO2 radicals in the atmosphere. 2014 , 53, 14596-600	147
769	Contrasting responses of silver birch VOC emissions to short- and long-term herbivory. 2014 , 34, 241-52	27
768	Observations of new particle formation at two distinct Indian subcontinental urban locations. 2014 , 96, 370-379	45
767	Atmospheric science: Involatile particles from rapid oxidation. 2014 , 506, 442-3	10
766	UV polarization lidar for remote sensing new particles formation in the atmosphere. 2014 , 22 Suppl 3, A1009-22	14
765	Water and formic acid aggregates: a molecular dynamics study. 2014 , 141, 104701	9
764	Positively Charged Phosphorus as a Hydrogen Bond Acceptor. 2014 , 5, 4225-31	82
763	Number and size distribution of airborne nanoparticles during summertime in Kuwait: first observations from the Middle East. 2014 , 48, 13634-43	25
762	Insight into acid-base nucleation experiments by comparison of the chemical composition of positive, negative, and neutral clusters. 2014 , 48, 13675-84	40
761	New Particle Formation and Growth in an Isoprene-Dominated Ozark Forest: From Sub-5 nm to CCN-Active Sizes. 2014 , 48, 1285-1298	28
760	Characterisation of organic contaminants in the CLOUD chamber at CERN. 2014 , 7, 2159-2168	32
759	The charging of neutral dimethylamine and dimethylamine-sulphuric acid clusters using protonated acetone. 2014 ,	
758	Changes in biogeochemistry and carbon fluxes in a boreal forest after the clear-cutting and partial burning of slash. 2014 , 188, 33-44	58
757	Changes in concentration of nitrogen-containing compounds in 10nm particles of boreal forest atmosphere at snowmelt. 2014 , 70, 1-10	5

(2014-2014)

756	Chemistry of atmospheric nucleation: on the recent advances on precursor characterization and atmospheric cluster composition in connection with atmospheric new particle formation. 2014 , 65, 21-37	178
755	Estimating atmospheric nucleation rates from size distribution measurements: Analytical equations for the case of size dependent growth rates. 2014 , 69, 13-20	12
754	Oxidation products of biogenic emissions contribute to nucleation of atmospheric particles. <i>Science</i> , 2014 , 344, 717-21	375
753	Infrequent occurrence of new particle formation at a semi-rural location, Gadanki, in tropical Southern India. 2014 , 94, 264-273	20
75 ²	Ultrafine particles in cities. 2014 , 66, 1-10	374
751	Infrared studies of the reaction of methanesulfonic acid with trimethylamine on surfaces. 2014 , 48, 323-30	15
750	High-Resolution Mobility and Mass Spectrometry of Negative Ions Produced in a 241Am Aerosol Charger. 2014 , 48, 261-270	32
749	Neutral molecular cluster formation of sulfuric acid-dimethylamine observed in real time under atmospheric conditions. 2014 , 111, 15019-24	155
748	The Biogeochemical Impacts of Forests and the Implications for Climate Change Mitigation. 2014,	
747	Observations on the formation, growth and chemical composition of aerosols in an urban environment. 2014 , 48, 6588-96	16
746	Growth rates of atmospheric molecular clusters based on appearance times and collision appearance fluxes: Growth by monomers. 2014 , 78, 55-70	12
745	An iodide-adduct high-resolution time-of-flight chemical-ionization mass spectrometer: application to atmospheric inorganic and organic compounds. 2014 , 48, 6309-17	288
744	Computational approaches for efficiently modelling of small atmospheric clusters. 2014 , 615, 26-29	53
743	Computational study of the Rayleigh light scattering properties of atmospheric pre-nucleation clusters. 2014 , 16, 10883-90	24
742	Theoretical study on stable small clusters of oxalic acid with ammonia and water. 2014 , 118, 1451-68	33
741	Measurement of sub-2 nm clusters of pristine and composite metal oxides during nanomaterial synthesis in flame aerosol reactors. 2014 , 86, 7523-9	22
740	Hydration of the sulfuric acid-methylamine complex and implications for aerosol formation. 2014 , 118, 7430-41	43
739	Number size distribution of aerosols at Mt. Huang and Nanjing in the Yangtze River Delta, China: Effects of air masses and characteristics of new particle formation. 2014 , 150, 42-56	38

738	Aerosol fast flow reactor for laboratory studies of new particle formation. 2014 , 78, 30-40	17
737	The formation of highly oxidized multifunctional products in the ozonolysis of cyclohexene. 2014 , 136, 15596-606	187
736	Recycling concrete: An undiscovered source of ultrafine particles. 2014 , 90, 51-58	28
735	Enhancement of the hygroscopicity parameter kappa of rural aerosols in northern Taiwan by anthropogenic emissions. 2014 , 84, 78-87	16
734	Benchmarking ab initio binding energies of hydrogen-bonded molecular clusters based on FTIR spectroscopy. 2014 , 118, 5316-22	48
733	Molecular interaction of pinic acid with sulfuric acid: exploring the thermodynamic landscape of cluster growth. 2014 , 118, 7892-900	57
732	Ice crystallization in ultrafine water-salt aerosols: nucleation, ice-solution equilibrium, and internal structure. 2014 , 136, 8081-93	53
731	Single-nanocrystal reaction trajectories reveal sharp cooperative transitions. 2014 , 14, 987-92	45
730	The effect of fluorine substitution in alcohol-amine complexes. 2014 , 16, 22882-91	57
729	Sub-3 nm particles observed at the coastal and continental sites in the United States. 2014 , 119, 860-879	22
729 728	Sub-3 nm particles observed at the coastal and continental sites in the United States. 2014 , 119, 860-879 A large source of low-volatility secondary organic aerosol. 2014 , 506, 476-9	1078
728	A large source of low-volatility secondary organic aerosol. 2014 , 506, 476-9 Suppression of new particle formation from monoterpene oxidation by	1078
728 727	A large source of low-volatility secondary organic aerosol. 2014 , 506, 476-9 Suppression of new particle formation from monoterpene oxidation by NO_x. 2014 , 14, 2789-2804 Impacts of new particle formation on aerosol cloud condensation nuclei (CCN) activity in Shanghai:	1078 51
728 727 726	A large source of low-volatility secondary organic aerosol. 2014, 506, 476-9 Suppression of new particle formation from monoterpene oxidation by NO _x . 2014, 14, 2789-2804 Impacts of new particle formation on aerosol cloud condensation nuclei (CCN) activity in Shanghai: case study. 2014, 14, 11353-11365	1078 51 27
728 727 726 725	A large source of low-volatility secondary organic aerosol. 2014, 506, 476-9 Suppression of new particle formation from monoterpene oxidation by NO _x . 2014, 14, 2789-2804 Impacts of new particle formation on aerosol cloud condensation nuclei (CCN) activity in Shanghai: case study. 2014, 14, 11353-11365 Molecular constraints on particle growth during new particle formation. 2014, 41, 6045-6054	1078 51 27 24
728 727 726 725 724	A large source of low-volatility secondary organic aerosol. 2014, 506, 476-9 Suppression of new particle formation from monoterpene oxidation by NO _x x 2014, 14, 2789-2804 Impacts of new particle formation on aerosol cloud condensation nuclei (CCN) activity in Shanghai: case study. 2014, 14, 11353-11365 Molecular constraints on particle growth during new particle formation. 2014, 41, 6045-6054 Polluted dust promotes new particle formation and growth. 2014, 4, 6634 Submicron aerosols at thirteen diversified sites in China: size distribution, new particle formation	1078 51 27 24 104

720	Modeling ultrafine particle growth at a pine forest site influenced by anthropogenic pollution during BEACHON-RoMBAS 2011. 2014 , 14, 11011-11029	9
719	Analysis of nucleation events in the European boundary layer using the regional aerosoldlimate model REMO-HAM with a solar radiation-driven OH-proxy. 2014 , 14, 11711-11729	11
718	Forest canopy interactions with nucleation mode particles. 2014 , 14, 11985-11996	12
717	Chemical composition and mass size distribution of PM₁ at an elevated site in central east China. 2014 , 14, 12237-12249	38
716	Aerosols and nucleation in eastern China: first insights from the new SORPES-NJU station. 2014 , 14, 2169-218	33 63
715	The direct and indirect radiative effects of biogenic secondary organic aerosol. 2014 , 14, 447-470	146
714	A naming convention for atmospheric organic aerosol. 2014 , 14, 5825-5839	68
713	Chemistry of new particle growth in mixed urban and biogenic emissions [Insights from CARES. 2014 , 14, 6477-6494	42
712	Hygroscopic properties of newly formed ultrafine particles at an urban site surrounded by deciduous forest (Sapporo, northern Japan) during the summer of 2011. 2014 , 14, 7519-7531	4
711	Spatial extension of nucleating air masses in the Carpathian Basin. 2014 , 14, 8841-8848	18
710	Climatology of new particle formation at Iza â mountain GAW observatory in the subtropical North Atlantic. 2014 , 14, 3865-3881	27
709	Enhancement of atmospheric H ₂ SO ₄ / H₂O nucleation: organic oxidation products versus amines. 2014 , 14, 751-764	42
708	Production and growth of new particles during two cruise campaigns in the marginal seas of China. 2014 , 14, 7941-7951	20
707	Electrical charging changes the composition of sulfuric acidammonia/dimethylamine clusters. 2014 , 14, 7995-8007	47
706	Growth of ice nanoparticles via uptake of individual molecules: pickup cross sections. 2014 , 488, 102016	
7°5	Schnelle Autoxidation bildet hochoxidierte RO2-Radikale in der AtmosphEe. 2014 , 126, 14825-14829	7
704	Mixing state and hygroscopicity of dust and haze particles before leaving Asian continent. 2014 , 119, 1044-1059	52
703	Reevaluating the contribution of sulfuric acid and the origin of organic compounds in atmospheric nanoparticle growth. 2015 , 42, 10,486	21

702	Organic aerosol processing in tropical deep convective clouds: Development of a new model (CRM-ORG) and implications for sources of particle number. 2015 , 120, 10,441	12
701	Extrapolating particle concentration along the size axis in the nanometer size range requires discrete rate equations. 2015 , 90, 1-13	3
700	On the properties and atmospheric implication of amine-hydrated clusters. 2015 , 5, 91500-91515	11
699	Introduction: The Pan-Eurasian Experiment (PEEX) Imultidisciplinary, multiscale and multicomponent research and capacity-building initiative. 2015 , 15, 13085-13096	35
698	Contribution from biogenic organic compounds to particle growth during the 2010 BEACHON-ROCS campaign in a Colorado temperate needleleaf forest. 2015 , 15, 8643-8656	11
697	Strong atmospheric new particle formation in winter in urban Shanghai, China. 2015 , 15, 1769-1781	116
696	Major contribution of neutral clusters to new particle formation at the interface between the boundary layer and the free troposphere. 2015 , 15, 3413-3428	32
695	Total sulfate vs. sulfuric acid monomer concenterations in nucleation studies. 2015 , 15, 3429-3443	15
694	Formation of highly oxidized multifunctional compounds: autoxidation of peroxy radicals formed in the ozonolysis of alkenes deduced from structureproduct relationships. 2015 , 15, 6745-6765	134
693	Experimental investigation of ionIbn recombination under atmospheric conditions. 2015, 15, 7203-7216	33
692	Particulate matter, air quality and climate: lessons learned and future needs. 2015 , 15, 8217-8299	462
691	Airborne measurements of new particle formation in the free troposphere above the Mediterranean Sea during the HYMEX campaign. 2015 , 15, 10203-10218	29
690	Thermodynamics of the formation of sulfuric acid dimers in the binary (H ₂ 5O ₄ H ₂ O) and ternary (H ₂ ONH ₃ 442ONH _{3<td>22 ;)</td>}	22 ;)
689	system. 2015 , 15, 10701-10721 Relating the hygroscopic properties of submicron aerosol to both gas- and particle-phase chemical composition in a boreal forest environment. 2015 , 15, 11999-12009	10
688	Biotic stress accelerates formation of climate-relevant aerosols in boreal forests. 2015 , 15, 12139-12157	40
687	Technical note: New particle formation event forecasts during PEGASOSIZeppelin Northern mission 2013 in Hyytil Finland. 2015 , 15, 12385-12396	14
686	Impact of gas-to-particle partitioning approaches on the simulated radiative effects of biogenic secondary organic aerosol. 2015 , 15, 12989-13001	28
685	Insights into the growth of newly formed particles in a subtropical urban environment. 2015 , 15, 13475-13485	3

(2015-2015)

684	Aerosol size distribution and new particle formation in the western Yangtze River Delta of China: 2 years of measurements at the SORPES station. 2015 , 15, 12445-12464	77
683	Size-resolved cloud condensation nuclei concentration measurements in the Arctic: two case studies from the summer of 2008. 2015 , 15, 13803-13817	8
682	On the derivation of particle nucleation rates from experimental formation rates. 2015 , 15, 4063-4075	25
681	Elemental composition and clustering behaviour of pinene oxidation products for different oxidation conditions. 2015 , 15, 4145-4159	14
680	Iodine observed in new particle formation events in the Arctic atmosphere during ACCACIA. 2015 , 15, 5599-5609	76
679	Technical Note: Using DEG-CPCs at upper tropospheric temperatures. 2015 , 15, 7547-7555	11
678	Atmospheric ions and new particle formation events at a tropical location, Pune, India. 2015 , 141, 3140-3156	17
677	Geographical and diurnal features of amine-enhanced boundary layer nucleation. 2015 , 120, 9606-9624	24
676	Ideas and perspectives: on the emission of amines from terrestrial vegetation in the context of new atmospheric particle formation. 2015 , 12, 3225-3240	16
675	A Review of Aerosol Nanoparticle Formation from Ions. 2015 , 32, 57-74	11
674	The charging of neutral dimethylamine and dimethylamineBulfuric acid clusters using protonated acetone. 2015 , 8, 2577-2588	1
673	Ultrafine particles over Eastern Australia: an airborne survey. 2015 , 67, 25308	15
672	Production of extremely low volatile organic compounds from biogenic emissions: Measured yields and atmospheric implications. 2015 , 112, 7123-8	260
671	On the composition of ammoniaBulfuric-acid ion clusters during aerosol particle formation. 2015 , 15, 55-78	68
670	Role of ammonia in forming secondary aerosols from gasoline vehicle exhaust. 2015 , 58, 1377-1384	26
669	Sub-3 nm Particle Detection with Commercial TSI 3772 and Airmodus A20 Fine Condensation Particle Counters. 2015 , 49, 674-681	24
668	Concentration, Size Distribution, and Formation of Trimethylaminium and Dimethylaminium Ions in Atmospheric Particles over Marginal Seas of China*. 2015 , 72, 3487-3498	24
667	Fragmentation of HClWater clusters upon ionization: Non-adiabatic ab initio dynamics study. 2015 , 622, 80-85	15

666	Characteristics of new particle formation events in Nanjing, China: Effect of water-soluble ions. 2015 , 108, 32-40	27
665	The molecular identification of organic compounds in the atmosphere: state of the art and challenges. 2015 , 115, 3919-83	300
664	Sulfuric acid nucleation: An experimental study of the effect of seven bases. 2015 , 120, 1933-1950	123
663	Highly Oxidized Multifunctional Organic Compounds Observed in Tropospheric Particles: A Field and Laboratory Study. 2015 , 49, 7754-61	110
662	Nature of CTAB/Water/Chloroform Reverse Micelles at Above- and Subzero Temperatures Studied by NMR and Molecular Dynamics Simulations. 2015 , 31, 8284-93	13
661	Field measurements of biogenic volatile organic compounds in the atmosphere by dynamic solid-phase microextraction and portable gas chromatography-mass spectrometry. 2015 , 115, 214-222	25
660	Reactivity of Hydrated Electron in Finite Size System: Sodium Pickup on Mixed N2O-Water Nanoparticles. 2015 , 6, 2865-9	17
659	An approach to investigate new particle formation in the vertical direction on the basis of high time-resolution measurements at ground level and sea level. 2015 , 102, 366-375	10
658	Techniques and instruments used for real-time analysis of atmospheric nanoscale molecular clusters: A review. 2015 , 1, 33-38	6
657	Comparison of daytime and nighttime new particle growth at the HKUST supersite in Hong Kong. 2015 , 49, 7170-8	24
656	Modeling the Charging of Highly Oxidized Cyclohexene Ozonolysis Products Using Nitrate-Based Chemical Ionization. 2015 , 119, 6339-45	63
655	Properties and Atmospheric Implication of Methylamine-Sulfuric Acid-Water Clusters. 2015 , 119, 8657-66	34
654	Computational Study of the Clustering of a Cyclohexene Autoxidation Product C6H8O7 with Itself and Sulfuric Acid. 2015 , 119, 8414-21	37
653	New particle formation at ground level and in the vertical column over the Barcelona area. 2015 , 164-165, 118-130	29
652	A long-term study of new particle formation in a coastal environment: meteorology, gas phase and solar radiation implications. 2015 , 511, 723-37	16
651	Rayleigh light scattering properties of atmospheric molecular clusters consisting of sulfuric acid and bases. 2015 , 17, 15701-9	9
650	Scanning supersaturation condensation particle counter applied as a nano-CCN counter for size-resolved analysis of the hygroscopicity and chemical composition of nanoparticles. 2015 , 8, 2161-2172	14
649	Roles of SO2 oxidation in new particle formation events. 2015 , 30, 90-101	7

648	Chemistry and the Linkages between Air Quality and Climate Change. 2015, 115, 3856-97	205
647	Implications of ammonia emissions from post-combustion carbon capture for airborne particulate matter. 2015 , 49, 5142-50	8
646	Sulphuric acid and aerosol particle production in the vicinity of an oil refinery. 2015, 119, 156-166	25
645	Images and properties of individual nucleated particles. 2015 , 123, 166-170	5
644	Gas Phase Detection of the NH-P Hydrogen Bond and Importance of Secondary Interactions. 2015 , 119, 10988-98	47
643	Sizing of neutral sub 3nm tungsten oxide clusters using Airmodus Particle Size Magnifier. 2015 , 87, 53-62	32
642	Hydration of a sulfuric acidඕxalic acid complex: acid dissociation and its atmospheric implication. 2015 , 5, 48638-48646	43
641	Insights into the Formation and Evolution of Individual Compounds in the Particulate Phase during Aromatic Photo-Oxidation. 2015 , 49, 13168-78	28
640	Growth of Ammonium Bisulfate Clusters by Adsorption of Oxygenated Organic Molecules. 2015 , 119, 11191-8	11
639	Organic Emissions from a Wood Stove and a Pellet Stove Before and After Simulated Atmospheric Aging. 2015 , 49, 1037-1050	26
638	Structures, Hydration, and Electrical Mobilities of Bisulfate Ion-Sulfuric Acid-Ammonia/Dimethylamine Clusters: A Computational Study. 2015 , 119, 9670-9	28
637	New particle formation and growth from methanesulfonic acid, trimethylamine and water. 2015 , 17, 13699-709	67
636	Development of a new corona discharge based ion source for high resolution time-of-flight chemical ionization mass spectrometer to measure gaseous H 2 SO 4 and aerosol sulfate. 2015 , 119, 167-173	14
635	Connection of organics to atmospheric new particle formation and growth at an urban site of Beijing. 2015 , 103, 7-17	43
634	Measurement of atmospheric amines and ammonia using the high resolution time-of-flight chemical ionization mass spectrometry. 2015 , 102, 249-259	97
633	Cryogenic ion trap vibrational spectroscopy of hydrogen-bonded clusters relevant to atmospheric chemistry. 2015 , 34, 1-34	140
632	Ultrafine particles over Germany 🗈 aerial survey. 2016 , 68, 29250	7
631	Growth of atmospheric clusters involving cluster-cluster collisions: comparison of different growth rate methods. 2016 ,	

630 Simple proxies for estimating the concentrations of monoterpenes and their oxidation products at a boreal forest site. **2016**,

629	From ionising radiation to air ion formation in the lower atmosphere. 2016 ,	
628	Measurements of biogenic volatile organic compounds at a grazed savannah-grassland-agriculture landscape in South Africa. 2016 ,	1
627	A global view on atmospheric concentrations of sub-3 nm particles measured with the Particle Size Magnifier. 2016 ,	1
626	Vertical and horizontal variation of aerosol number size distribution in the boreal environment. 2016 ,	12
625	Long-term analysis of clear-sky new particle formation events and non-events in Hyyti ©2016 ,	
624	Challenges associated with the sampling and analysis of organosulfur compounds in air using real-time PTR-ToF-MS and offline GC-FID. 2016 , 9, 1325-1340	20
623	How to reliably detect molecular clusters and nucleation mode particles with Neutral cluster and Air Ion Spectrometer (NAIS). 2016 , 9, 3577-3605	30
622	Modelling the dispersion of particle numbers in five European cities. 2016 , 9, 451-478	33
621	Coupling an aerosol box model with one-dimensional flow: a tool for understanding observations of new particle formation events. 2016 , 68, 29706	14
620	A laser-induced fluorescence instrument for aircraft measurements of sulfur dioxide in the upper troposphere and lower stratosphere. 2016 , 9, 4601-4613	15
619	. 2016,	20
618	A new high-transmission inlet for the Caltech nano-RDMA for size distribution measurements of sub-3 nm ions at ambient concentrations. 2016 , 9, 2709-2720	13
617	Potential of needle trap microextractionportable gas chromatographythass spectrometry for measurement of atmospheric volatile compounds. 2016 , 9, 3661-3671	13
616	Operation of the Airmodus A11 nano Condensation Nucleus Counter at various inlet pressures and various operation temperatures, and design of a new inlet system. 2016 , 9, 2977-2988	28
615	Ion mobility spectrometryhass spectrometry (IMSMS) for on- and offline analysis of atmospheric gas and aerosol species. 2016 , 9, 3245-3262	42
614	BAECC: A Field Campaign to Elucidate the Impact of Biogenic Aerosols on Clouds and Climate. 2016 , 97, 1909-1928	57
613	Effect of ions on sulfuric acid-water binary particle formation: 2. Experimental data and comparison with QC-normalized classical nucleation theory. 2016 , 121, 1752-1775	80

	Spiers Memorial Lecture. Introductory lecture: chemistry in the urban atmosphere. 2016 , 189, 9-29	5
611	Hydroxyl radical-induced formation of highly oxidized organic compounds. 2016 , 7, 13677	124
610	Effect of dimethylamine on the gas phase sulfuric acid concentration measured by Chemical Ionization Mass Spectrometry. 2016 , 121, 3036-3049	13
609	Experimental particle formation rates spanning tropospheric sulfuric acid and ammonia abundances, ion production rates, and temperatures. 2016 , 121, 12,377	54
608	Droplet formation and growth inside a polymer network: A molecular dynamics simulation study. 2016 , 144, 134502	9
607	Enhanced Volatile Organic Compounds emissions and organic aerosol mass increase the oligomer content of atmospheric aerosols. 2016 , 6, 35038	64
606	Isoprene suppression of new particle formation: Potential mechanisms and implications. 2016 , 121, 14,621	26
605	The role of low-volatility organic compounds in initial particle growth in the atmosphere. 2016 , 533, 527-31	388
604	Atmospheric science: Unexpected player in particle formation. 2016 , 533, 478-9	12
603	Ion-induced nucleation of pure biogenic particles. 2016 , 533, 521-6	377
602	New particle formation in the free troposphere: A question of chemistry and timing. <i>Science</i> , 2016 , 352, 1109-12	264
602		
	352, 1109-12	264
601	33.3 Infrared spectroscopic probing of dimethylamine clusters in an Ar matrix. 2016, 40, 51-9 Theoretical investigation of the hydrogen bond interactions of methanol and dimethylamine with	264 16
600	33.3 Infrared spectroscopic probing of dimethylamine clusters in an Ar matrix. 2016, 40, 51-9 Theoretical investigation of the hydrogen bond interactions of methanol and dimethylamine with hydrazone and its derivatives. 2016, 27, 1241-1253 Reactions of Atmospheric Particulate Stabilized Criegee Intermediates Lead to	264 16 11
600 599	Infrared spectroscopic probing of dimethylamine clusters in an Ar matrix. 2016, 40, 51-9 Theoretical investigation of the hydrogen bond interactions of methanol and dimethylamine with hydrazone and its derivatives. 2016, 27, 1241-1253 Reactions of Atmospheric Particulate Stabilized Criegee Intermediates Lead to High-Molecular-Weight Aerosol Components. 2016, 50, 5702-10	264 16 11 43
600 599 598	Infrared spectroscopic probing of dimethylamine clusters in an Ar matrix. 2016, 40, 51-9 Theoretical investigation of the hydrogen bond interactions of methanol and dimethylamine with hydrazone and its derivatives. 2016, 27, 1241-1253 Reactions of Atmospheric Particulate Stabilized Criegee Intermediates Lead to High-Molecular-Weight Aerosol Components. 2016, 50, 5702-10 Diurnal patterns in Scots pine stem oleoresin pressure in a boreal forest. 2016, 39, 527-38 Deprotonated Dicarboxylic Acid Homodimers: Hydrogen Bonds and Atmospheric Implications. 2016	264 16 11 43

594	Ion mobility spectrometry-mass spectrometry examination of the structures, stabilities, and extents of hydration of dimethylamine-sulfuric acid clusters. 2016 , 18, 22962-72	30
593	Tip-Enhanced Raman Spectroscopy of Atmospherically Relevant Aerosol Nanoparticles. 2016 , 88, 9766-9772	31
592	How salt lakes affect atmospheric new particle formation: A case study in Western Australia. 2016 , 573, 985-995	4
591	Observation of aerosol size distribution and new particle formation at a coastal city in the Yangtze River Delta, China. 2016 , 565, 1175-1184	15
590	Emission, Transformation, and Fate of Nanoparticles in the Atmosphere. 2016 , 205-223	2
589	Intense secondary aerosol formation due to strong atmospheric photochemical reactions in summer: observations at a rural site in eastern Yangtze River Delta of China. 2016 , 571, 1454-66	72
588	Reduced anthropogenic aerosol radiative forcing caused by biogenic new particle formation. 2016 , 113, 12053-12058	79
587	Formation of the H2SO4 IHSOI dimer in the atmosphere as a function of conditions: a simulation study. 2016 , 114, 3475-3482	4
586	Ultrafine Particles Pollution and Measurements. 2016 , 73, 369-390	4
585	Long-term observation of air pollution-weather/climate interactions at the SORPES station: a review and outlook. 2016 , 10, 1	48
584	Aerosol Chemistry Resolved by Mass Spectrometry: Insights into Particle Growth after Ambient New Particle Formation. 2016 , 50, 10814-10822	16
583	Effect of Conformers on Free Energies of Atmospheric Complexes. 2016 , 120, 8613-8624	24
582	Theoretical Studies on Reactions of OH with H2SO4NH3 Complex and NH2 with H2SO4 in the Presence of Water. 2016 , 1, 1421-1430	15
581	Key features of new particle formation events at background sites in China and their influence on cloud condensation nuclei. 2016 , 10, 1	24
580	The influence of emission control on particle number size distribution and new particle formation during China's V-Day parade in 2015. 2016 , 573, 409-419	19
579	Molecular-scale evidence of aerosol particle formation via sequential addition of HIO. 2016 , 537, 532-534	155
578	Characteristics of dimethylaminium and trimethylaminium in atmospheric particles ranging from supermicron to nanometer sizes over eutrophic marginal seas of China and oligotrophic open oceans. 2016 , 572, 813-824	22
577	Hydrogen bonding in cyclic complexes of carboxylic acidBulfuric acid and their atmospheric implications. 2016 , 6, 71733-71743	23

576	A conceptual framework for mixing structures in individual aerosol particles. 2016 , 121, 13,784-13,798	78
575	Amazon boundary layer aerosol concentration sustained by vertical transport during rainfall. 2016 , 539, 416-419	83
574	Contribution of new particle formation to the total aerosol concentration at the high-altitude site Jungfraujoch (3580[m[asl, Switzerland). 2016 , 121, 11,692-11,711	14
573	Rupturing of Biological Spores As a Source of Secondary Particles in Amazonia. 2016 , 50, 12179-12186	32
572	Accurate thermodynamic properties of gas phase hydrogen bonded complexes. 2016 , 18, 23831-9	17
571	A chamber study of the influence of boreal BVOC emissions and sulfuric acid on nanoparticle formation rates at ambient concentrations. 2016 , 16, 1955-1970	6
570	Measurements of biogenic volatile organic compounds at a grazed savannah grassland agricultural landscape in South Africa. 2016 , 16, 15665-15688	22
569	Using satellite-based measurements to explore spatiotemporal scales and variability of drivers of new particle formation. 2016 , 121, 12217-12235	5
568	Source characterization of highly oxidized multifunctional compounds in a boreal forest environment using positive matrix factorization. 2016 , 16, 12715-12731	71
567	Observation of new particle formation and measurement of sulfuric acid, ammonia, amines and highly oxidized organic molecules at a rural site in central Germany. 2016 , 16, 12793-12813	51
566	Simple proxies for estimating the concentrations of monoterpenes and their oxidation products at a boreal forest site. 2016 , 16, 13291-13307	21
565	How do air ions reflect variations in ionising radiation in the lower atmosphere in a boreal forest?. 2016 , 16, 14297-14315	10
564	High concentrations of sub-3nm clusters and frequent new particle formation observed in the Po Valley, Italy, during the PEGASOS 2012 campaign. 2016 , 16, 1919-1935	18
563	Nucleation and growth of sub-3 nm particles in the polluted urban atmosphere of a megacity in China. 2016 , 16, 2641-2657	42
562	Molecular corridors and parameterizations of volatility in the chemical evolution of organic aerosols. 2016 , 16, 3327-3344	90
561	Observation of viscosity transition in <i></i>-pinene secondary organic aerosol. 2016 , 16, 4423-4438	47
560	Growth of atmospheric clusters involving cluster©luster collisions: comparison of different growth rate methods. 2016 , 16, 5545-5560	12
559	Synergistic use of Lagrangian dispersion and radiative transfer modelling with satellite and surface remote sensing measurements for the investigation of volcanic plumes: the Mount Etna eruption of 25½7[October 2013. 2016 , 16, 6841-6861	26

558	Using a combined power law and log-normal distribution model to simulate particle formation and growth in a mobile aerosol chamber. 2016 , 16, 7067-7090	3
557	Measurement, growth types and shrinkage of newly formed aerosol particles at an urban research platform. 2016 , 16, 7837-7851	28
556	Regional effect on urban atmospheric nucleation. 2016 , 16, 8715-8728	40
555	Indirect evidence of the composition of nucleation mode atmospheric particles in the high Arctic. 2016 , 121, 965-975	34
554	The versatile size analyzing nuclei counter (vSANC). 2016 , 50, 947-958	7
553	Quantitative analysis of aliphatic amines in urban aerosols based on online derivatization and high performance liquid chromatography. 2016 , 18, 796-801	10
552	Reactions of Methanesulfonic Acid with Amines and Ammonia as a Source of New Particles in Air. 2016 , 120, 1526-36	86
551	On secondary new particle formation in China. 2016 , 10, 1	39
550	Clustering of amines and hydrazines in atmospheric nucleation. 2016 , 472, 198-207	12
549	Incorporation of new particle formation and early growth treatments into WRF/Chem: Model improvement, evaluation, and impacts of anthropogenic aerosols over East Asia. 2016 , 124, 262-284	27
548	Approximate analytical solutions to the condensation-coagulation equation of aerosols. 2016 , 50, 578-590	1
547	Coupled Cluster Evaluation of the Stability of Atmospheric Acid-Base Clusters with up to 10 Molecules. 2016 , 120, 621-30	62
546	What Can the Kinetics of Amyloid Fibril Formation Tell about Off-pathway Aggregation?. 2016, 291, 2018-203	3233
545	The HO2 + (H2O)n + O3 reaction: an overview and recent developments. 2016 , 70, 1	9
544	Probing the early stages of solvation of cis-pinate dianions by water, acetonitrile, and methanol: a photoelectron spectroscopy and theoretical study. 2016 , 18, 3628-37	10
543	Can Highly Oxidized Organics Contribute to Atmospheric New Particle Formation?. 2016 , 120, 1452-8	30
542	Review on recent progress in observations, source identifications and countermeasures of PM2.5. 2016 , 86, 150-70	184
541	Dimethylamine Addition to Formaldehyde Catalyzed by a Single Water Molecule: A Facile Route for Atmospheric Carbinolamine Formation and Potential Promoter of Aerosol Growth. 2016 , 120, 1358-68	26

(2017-2017)

540	Cluster Model Studies of Anion and Molecular Specificities via Electrospray Ionization Photoelectron Spectroscopy. 2017 , 121, 1389-1401	37
539	The high charge fraction of flame-generated particles in the size range below 3 nm measured by enhanced particle detectors. 2017 , 176, 72-80	24
538	Oxygenate-Induced Tuning of Aldehyde-Amine Reactivity and Its Atmospheric Implications. 2017 , 121, 1022-1031	11
537	The Role of Oxalic Acid in New Particle Formation from Methanesulfonic Acid, Methylamine, and Water. 2017 , 51, 2124-2130	38
536	Atmospheric gas-to-particle conversion: why NPF events are observed in megacities?. 2017, 200, 271-288	84
535	Global sources, emissions, transport and deposition of dust and sand and their effects on the climate and environment: a review. 2017 , 11, 1	26
534	Forecasting ultrafine particle concentrations from satellite and in situ observations. 2017, 122, 1828-1837	4
533	Regional and local new particle formation events observed in the Yangtze River Delta region, China. 2017 , 122, 2389-2402	31
532	Hygroscopic properties of urban aerosols and their cloud condensation nuclei activities measured in Seoul during the MAPS-Seoul campaign. 2017 , 153, 217-232	17
531	Contribution of methane sulfonic acid to new particle formation in the atmosphere. 2017 , 174, 689-699	40
530	First measurements of the number size distribution of 1½ nm aerosol particles released from manufacturing processes in a cleanroom environment. 2017 , 51, 685-693	9
529	Laboratory observations of temperature and humidity dependencies of nucleation and growth rates of sub-3 nm particles. 2017 , 122, 1919-1929	20
528	Solar eclipse demonstrating the importance of photochemistry in new particle formation. 2017 , 7, 45707	25
527	Structures and energetics of hydrated deprotonated cis-pinonic acid anion clusters and their atmospheric relevance. 2017 , 19, 10676-10684	14
526	Atmospheric Aerosols: Clouds, Chemistry, and Climate. 2017 , 8, 427-444	50
525	Production of neutral molecular clusters by controlled neutralization of mobility standards. 2017 , 51, 946-955	5
524	Effect of Bisulfate, Ammonia, and Ammonium on the Clustering of Organic Acids and Sulfuric Acid. 2017 , 121, 4812-4824	28
523	Cluster formation mechanisms of titanium dioxide during combustion synthesis: Observation with an APi-TOF. 2017 , 51, 1071-1081	13

522	What Is Required for Highly Oxidized Molecules To Form Clusters with Sulfuric Acid?. 2017, 121, 4578-4587	43
521	Introductory lecture: atmospheric chemistry in the Anthropocene. 2017 , 200, 11-58	15
520	Ambient observations of dimers from terpene oxidation in the gas phase: Implications for new particle formation and growth. 2017 , 44, 2958-2966	54
519	Hydrogen bond docking site competition in methyl esters. 2017 , 181, 122-130	9
518	Proton Transfer in Mixed Clusters of Methanesulfonic Acid, Methylamine, and Oxalic Acid: Implications for Atmospheric Particle Formation. 2017 , 121, 2377-2385	29
517	Subtle differences in the hydrogen bonding of alcohol to divalent oxygen and sulfur. 2017 , 667, 146-153	28
516	Atmospheric implication of the hydrogen bonding interaction in hydrated clusters of HONO and dimethylamine in the nighttime. 2017 , 19, 65-77	13
515	Basis set convergence of the binding energies of strongly hydrogen-bonded atmospheric clusters. 2017 , 19, 1122-1133	55
514	Condensation in One-Dimensional Dead-End Nanochannels. 2017, 11, 304-313	41
513	Highly Oxygenated Molecules from Atmospheric Autoxidation of Hydrocarbons: A Prominent Challenge for Chemical Kinetics Studies. 2017 , 49, 821-831	32
512	Direct observation of new particle formation during ozonolysis of isoprene and ethene competing against the growth of preexisting particles. 2017 , 170, 149-155	5
511	Elucidating the Limiting Steps in Sulfuric Acid-Base New Particle Formation. 2017 , 121, 8288-8295	35
510	Particle formation and growth from oxalic acid, methanesulfonic acid, trimethylamine and water: a combined experimental and theoretical study. 2017 , 19, 28286-28301	30
509	New Particle Formation and Growth Mechanisms in Highly Polluted Environments. 2017, 3, 245-253	28
508	The growth mechanism of sulfuric acid clusters: Implication for the formation of cloud condensation nuclei. 2017 , 114, 169-179	3
507	The Influence of the Position of the Double Bond and Ring Size on the Stability of Hydrogen Bonded Complexes. 2017 , 7, 11310	14
506	Infrared-Vacuum Ultraviolet Spectroscopic and Theoretical Study of Neutral Methylamine Dimer. 2017 , 121, 7176-7182	15
505	Dimethyl Sulfoxide Complexes Detected at Ambient Conditions. 2017 , 121, 6046-6053	5

504	Basin-Scale Observations of Monoterpenes in the Arctic and Atlantic Oceans. 2017, 51, 10449-10458	10
503	A tunable high-pass filter for simple and inexpensive size-segregation of sub-10-nm nanoparticles. 2017 , 7, 45678	5
502	On the sources of uncertainty in the sub-3 nm particle concentration measurement. 2017 , 112, 34-51	23
501	The effect of sub-zero temperature on the formation and composition of secondary organic aerosol from ozonolysis of alpha-pinene. 2017 , 19, 1220-1234	18
500	Molecular understanding of the interaction of methyl hydrogen sulfate with ammonia/dimethylamine/water. 2017 , 186, 331-340	13
499	Nanoparticles grown from methanesulfonic acid and methylamine: microscopic structures and formation mechanism. 2017 , 19, 31949-31957	8
498	Mechanisms of Atmospherically Relevant Cluster Growth. 2017 , 50, 1965-1975	28
497	Revealing isomerism in sodium-water clusters: Photoionization spectra of Na(HO) (n = 2-90). 2017 , 146, 244303	6
496	C1-C2 alkyl aminiums in urban aerosols: Insights from ambient and fuel combustion emission measurements in the Yangtze River Delta region of China. 2017 , 230, 12-21	18
495	Laboratory verification of Aerosol Diffusion Spectrometer and the application to ambient measurements of new particle formation. 2017 , 105, 10-23	16
494	Emission of 1.3🗓0 nm airborne particles from brake materials. 2017, 51, 91-96	42
493	Characterization of particle number size distribution and new particle formation in Southern China. 2017 , 51, 342-351	11
492	Understanding aerosol formation mechanisms in a subtropical atmosphere impacted by biomass burning and agroindustry. 2017 , 183, 94-103	7
491	Observation of incipient particle formation during flame synthesis by tandem differential mobility analysis-mass spectrometry (DMA-MS). 2017 , 36, 745-752	20
490	Characterization of particle number size distribution and new particle formation in an urban environment in Lanzhou, China. 2017 , 103, 53-66	16
489	Nucleation of Polyaniline Microspheres and Interconnected Nanostructures from Strongly Coupled Micelle-like Systems. 2017 , 121, 28506-28514	3
488	Perspective: Aerosol microphysics: From molecules to the chemical physics of aerosols. 2017 , 147, 220901	30
487	Features in air ions measured by an air ion spectrometer (AIS) at Dome C. 2017, 17, 13783-13800	8

486	The role of highly oxygenated molecules (HOMs) in determining the composition of ambient ions in the boreal forest. 2017 , 17, 13819-13831	34
485	The role of ions in new particle formation in the CLOUD chamber. 2017 , 17, 15181-15197	32
484	Measurements of sub-3 nm particles using a particle size magnifier in different environments: from clean mountain top to polluted megacities. 2017 , 17, 2163-2187	56
483	Hygroscopic properties of aminium sulfate aerosols. 2017 , 17, 4369-4385	10
482	Simultaneous measurements of new particle formation at 1 s time resolution at a street site and a rooftop site. 2017 , 17, 9469-9484	14
481	Aerosol surface area concentration: a governing factor in new particle formation in Beijing. 2017 , 17, 12327-12340	52
480	A new balance formula to estimate new particle formation rate: reevaluating the effect of coagulation scavenging. 2017 , 17, 12659-12675	29
479	Estimation of atmospheric particle formation rates through an analytical formula: validation and application in Hyytilland Puijo, Finland. 2017 , 17, 13361-13371	1
478	Quantification of an atmospheric nucleation and growth process as labingle source of aerosol particles in a city. 2017 , 17, 15007-15017	10
477	Long-term analysis of clear-sky new particle formation events and nonevents in Hyyti [I]2017 , 17, 6227-6241	55
476	Heterogeneous uptake of ammonia and dimethylamine into sulfuric and oxalic acid particles. 2017 , 17, 6323-6339	14
475	Modeling the role of highly oxidized multifunctional organicImolecules for the growth of new particles overItheIborealIforestIregion. 2017 , 17, 8887-8901	22
474	Infrared-Vacuum Ultraviolet Spectroscopic and Theoretical Study of Neutral Trimethylamine Dimer 2017 , 30, 691-695	2
473	Aerosol Surface Area Concentration: a Governing Factor for New Particle Formation in Beijing. 2017	
472	8. Evaporation of droplets. The Kelvin and the coffee-stain effects. 2017 , 119-137	
472 471	8. Evaporation of droplets. The Kelvin and the coffee-stain effects. 2017 , 119-137 Environmental analysis: Atmospheric samples. 2017 , 769-798	
		16

468	Quantitation of 11 alkylamines in atmospheric samples: separating structural isomers by ion chromatography. 2017 , 10, 1061-1078	15
467	Formation Mechanism of Atmospheric Ammonium Bisulfate: Hydrogen-Bond-Promoted Nearly Barrierless Reactions of SO with NH and H O. 2018 , 19, 967-972	8
466	Comparison of atmospheric new particle formation events in three Central European cities. 2018 , 178, 191-197	18
465	Effect of Residential Radon Decay Product Dose Factor Variability on Reporting of Dose. 2018 , 114, 398-407	9
464	The Silk Road agenda of the Pan-Eurasian Experiment (PEEX) program. 2018, 2, 8-35	5
463	Bildung von Aufbauprodukten aus den Selbst- und Kreuzreaktionen von RO2-Radikalen in der Atmosphle. 2018 , 130, 3882-3886	2
462	Guanidine: A Highly Efficient Stabilizer in Atmospheric New-Particle Formation. 2018, 122, 4717-4729	17
461	Vertically resolved concentration and liquid water content of atmospheric nanoparticles at the US DOE Southern Great Plains site. 2018 , 18, 311-326	21
460	Spatial distribution and occurrence probability of regional new particle formation events in eastern China. 2018 , 18, 587-599	20
459	Interaction of oxalic acid with methylamine and its atmospheric implications 2018, 8, 7225-7234	12
458	Evidence for Diverse Biogeochemical Drivers of Boreal Forest New Particle Formation. 2018 , 45, 2038-2046	16
457	Accretion Product Formation from Self- and Cross-Reactions of RO Radicals in the Atmosphere. 2018 , 57, 3820-3824	88
456	Novel insights on new particle formation derived from a pan-european observing system. 2018 , 8, 1482	34
455	A computational investigation of the sulphuric acid-catalysed 1,4-hydrogen transfer in higher Criegee intermediates. 2018 , 118, e25599	6
454	Current state of aerosol nucleation parameterizations for air-quality and climate modeling. 2018 , 179, 77-106	18
453	Closed-Shell Organic Compounds Might Form Dimers at the Surface of Molecular Clusters. 2018 , 122, 1771-1780	10
452	Temporal distribution and other characteristics of new particle formation events in an urban environment. 2018 , 233, 552-560	11
451	Enhancing the detection efficiency of condensation particle counters for sub-2 nm particles. 2018 , 117, 44-53	24

450	Atmospheric autoxidation is increasingly important in urban and suburban North America. 2018 , 115, 64-69	101
449	A density functional theory study of aldehydes and their atmospheric products participating in nucleation. 2018 , 20, 1005-1011	21
448	Air Pollution and Air Quality. 2018 , 151-176	7
447	Effect of Mixing Ammonia and Alkylamines on Sulfate Aerosol Formation. 2018 , 122, 1612-1622	40
446	Resolving nanoparticle growth mechanisms from size- and time-dependent growth rate analysis. 2018 , 18, 1307-1323	15
445	Nanoparticle growth by particle-phase chemistry. 2018 , 18, 1895-1907	15
444	Formation of highly oxygenated organic molecules from aromatic compounds. 2018, 18, 1909-1921	83
443	New particle formation in the sulfuric acidlimethylamine water system: reevaluation of CLOUD chamber measurements and comparison to an aerosol nucleation and growth model. 2018 , 18, 845-863	62
442	Influence of temperature on the molecular composition of ions and charged clusters during pure biogenic nucleation. 2018 , 18, 65-79	39
441	Observations of biogenic ion-induced cluster formation in the atmosphere. 2018 , 4, eaar5218	37
440	Hybridization of Nitrogen Determines Hydrogen-Bond Acceptor Strength: Gas-Phase Comparison of Redshifts and Equilibrium Constants. 2018 , 122, 3899-3908	7
439	Sub-2 nm particle measurement in high-temperature aerosol reactors: a review. 2018 , 21, 60-66	10
438	Synergistic Effect of Ammonia and Methylamine on Nucleation in the Earth's Atmosphere. A Theoretical Study. 2018 , 122, 3470-3479	27
437	Hydrogen bond docking preference in furans: OH?Ūs. OH?O. 2018 , 191, 155-164	15
436	Mass spectrometry of aerosol particle analogues in molecular beam experiments. 2018, 37, 630-651	38
435	A multicomponent kinetic model established for investigation on atmospheric new particle formation mechanism in HSO-HNO-NH-VOC system. 2018 , 616-617, 1414-1422	12
434	Combining airborne in situ and ground-based lidar measurements for attribution of aerosol layers. 2018 , 18, 10575-10591	6
433	Estimating the influence of transport on aerosol size distributions during new particle formation events. 2018 , 18, 16587-16599	10

432	Refined classification and characterization of atmospheric new-particle formation events using air ions. 2018 , 18, 17883-17893	23
431	Estimating the influence of transport to aerosol size distributions during new particle formation events. 2018 ,	
430	Over a ten-year record of aerosol optical properties at SMEAR II. 2018,	
429	Differentiating between particle formation and growth events in an urban environment. 2018,	
428	New Particle Formation at a High Altitude Site in India: Impact of Fresh Emissions and Long Range Transport. 2018 ,	1
427	Sesquiterpenes identified as key species for atmospheric chemistry in boreal forest by terpenoid and OVOC measurements. 2018 ,	1
426	Heterogeneous reactions of SO on the hematite(0001) surface. 2018 , 149, 194703	6
425	Driving parameters of biogenic volatile organic compounds and consequences on new particle formation observed at an eastern Mediterranean background site. 2018 , 18, 14297-14325	22
424	Amines in boreal forest air at SMEAR II station in Finland. 2018 , 18, 6367-6380	18
423	Impact of Multiphase Chemistry on Nanoparticle Growth and Composition. 2018, 9-34	
422	Direct Evidence for Curvature-Dependent Surface Tension in Capillary Condensation: Kelvin Equation at Molecular Scale. 2018 , 8,	25
421	A theoretical investigation on the structures of (NH3)[[H2SO4)[[H2O]0-14 clusters. 2018 , 119, e25850	1
420	Large Increases in Primary Trimethylaminium and Secondary Dimethylaminium in Atmospheric Particles Associated With Cyclonic Eddies in the Northwest Pacific Ocean. 2018 , 123, 12,133-12,146	9
419	Vertical characterization of highly oxygenated molecules (HOMs) below and above a boreal forest canopy. 2018 , 18, 17437-17450	18
418	Multicomponent new particle formation from sulfuric acid, ammonia, and biogenic vapors. 2018, 4, eaau5363	105
417	Combining airborne in situ and ground-based lidar measurements for attribution of aerosol layers. 2018 ,	
416	Ion-induced sulfuric acid-ammonia nucleation drives particle formation in coastal Antarctica. 2018 , 4, eaat9744	48
415	Long-term measurements of volatile organic compounds highlight the importance of sesquiterpenes for the atmospheric chemistry of a boreal forest. 2018 , 18, 13839-13863	46

414	Robust metric for quantifying the importance of stochastic effects on nanoparticle growth. 2018 , 8, 14160	8
413	Size-resolved hygroscopic behavior of atmospheric aerosols during heavy aerosol pollution episodes in Beijing in December 2016. 2018 , 194, 188-197	28
412	Characterization of a high-resolution supercritical differential mobility analyzer at reduced flow rates. 2018 , 52, 1332-1343	9
411	Atmospheric new particle formation and growth: review of field observations. 2018 , 13, 103003	192
410	Consequences of dynamic and timing properties of new aerosol particle formation and consecutive growth events. 2018 ,	
409	Exploring non-linear associations between atmospheric new-particle formation and ambient variables: a mutual information approach. 2018 , 18, 12699-12714	14
408	The role of H₂SO₄-NH₃ anion clusters in ion-induced aerosol nucleation mechanisms in the boreal forest. 2018 , 18, 13231-13243	19
407	Exploring the potential of nano-Killer theory to describe the growth of atmospheric molecular clusters by organic vapors using cluster kinetics simulations. 2018 , 18, 13733-13754	7
406	Modelling studies of HOMs and their contributions to new particle formation and growth: comparison of boreal forest in Finland and a polluted environment in China. 2018 , 18, 11779-11791	18
405	Current situation of atmospheric nanoparticles in Fukue Island, Japan. 2018 , 70, 1-12	1
404	Secondary organic aerosol formation from photooxidation of furan: effects of NO_x level and humidity. 2018 ,	3
403	Multi-year statistical and modeling analysis of submicrometer aerosol number size distributions at a rain forest site in Amazonia. 2018 , 18, 10255-10274	19
402	Multi-year statistical and modelling analysis of submicrometer aerosol number size distributions at a rain forest site in Amazonia. 2018 ,	
401	Vertical profiles of sub-3 nm particles over the boreal forest. 2018 ,	1
400	Accretion Product Formation from Ozonolysis and OH Radical Reaction of Pinene: Mechanistic Insight and the Influence of Isoprene and Ethylene. 2018 , 52, 11069-11077	48
399	Differentiating between particle formation and growth events in an urban environment. 2018 , 18, 11171-111	8 3
398	Refined classification and characterization of atmospheric new particle formation events using air ions. 2018 ,	
397	A unifying identity for the work of cluster formation in heterogeneous and homogeneous nucleation theory. 2018 , 149, 084702	4

(2018-2018)

Analysis of atmospheric visibility degradation in early haze based on the nucleation clustering model. 2018 , 193, 205-213	2
Direct Link between Structure and Hydration in Ammonium and Aminium Bisulfate Clusters Implicated in Atmospheric New Particle Formation. 2018 , 9, 5647-5652	17
Aerosols in atmospheric chemistry and biogeochemical cycles of nutrients. 2018 , 13, 063004	49
Ultrafine Particles in the Lower Troposphere: Major Sources, Invisible Plumes, and Meteorological Transport Processes. 2018 , 99, 2587-2602	13
Number size distribution of atmospheric particles in a suburban Beijing in the summer and winter of 2015. 2018 , 186, 32-44	9
Imaging nanobubble nucleation and hydrogen spillover during electrocatalytic water splitting. 2018 , 115, 5878-5883	74
Stabilities of protonated water-ammonia clusters. 2018 , 148, 184306	3
Direct Observation of Hierarchic Molecular Interactions Critical to Biogenic Aerosol Formation. 2018 , 1,	11
Infrared photodissociation spectroscopy of cold cationic trimethylamine complexes. 2018 , 20, 25583-25591	9
Laboratory verification of a new high flow differential mobility particle sizer, and field measurements in Hyyti III2018 , 124, 1-9	14
From O-Initiated SO Oxidation to Sulfate Formation in the Gas Phase. 2018 , 122, 5781-5788	8
Classification of the new particle formation events observed at a tropical site, Pune, India. 2018 , 190, 10-22	7
Particles in the Air. 2018 ,	1
Filtration of Sub-3.3 nm Tungsten Oxide Particles Using Nanofibrous Filters. 2018 , 11,	O
Simulation on different response characteristics of aerosol particle number concentration and mass concentration to emission changes over mainland China. 2018 , 643, 692-703	21
Revealing the Sources of Atmospheric Ammonia: a Review. 2018 , 4, 189-197	17
Atmospheric new particle formation from sulfuric acid and amines in a Chinese megacity. <i>Science</i> , 2018 , 361, 278-281	265
Ambient Measurements of Highly Oxidized Gas-Phase Molecules during the Southern Oxidant and Aerosol Study (SOAS) 2013. 2018 , 2, 653-672	37
	Direct Link between Structure and Hydration in Ammonium and Aminium Bisulfate Clusters Implicated in Atmospheric New Particle Formation. 2018, 9, 5647-5652 Aerosols in atmospheric chemistry and biogeochemical cycles of nutrients. 2018, 13, 063004 Ultrafine Particles in the Lower Troposphere: Major Sources, Invisible Plumes, and Meteorological Transport Processes. 2018, 99, 2587-2602 Number size distribution of atmospheric particles in a suburban Beijing in the summer and winter of 2015. 2018, 186, 32-44 Imaging nanobubble nucleation and hydrogen spillover during electrocatalytic water splitting. 2018, 115, 5878-5883 Stabilities of protonated water-ammonia clusters. 2018, 148, 184306 Direct Observation of Hierarchic Molecular Interactions Critical to Biogenic Aerosol Formation. 2018, 1, Infrared photodissociation spectroscopy of cold cationic trimethylamine complexes. 2018, 20, 25583-25591 Laboratory verification of a new high flow differential mobility particle sizer, and field measurements in Hytytilizo18, 124, 1-9 From O-Initiated SO Oxidation to Sulfate Formation in the Gas Phase. 2018, 122, 5781-5788 Classification of the new particle formation events observed at a tropical site, Pune, India. 2018, 190, 10-22 Particles in the Air. 2018. Filtration of Sub-3.3 nm Tungsten Oxide Particles Using Nanofibrous Filters. 2018, 11, Simulation on different response characteristics of aerosol particle number concentration and mass concentration to emission changes over mainland China. 2018, 643, 692-703 Revealing the Sources of Atmospheric Ammonia: a Review. 2018, 4, 189-197 Atmospheric new particle formation from sulfuric acid and amines in a Chinese megacity. Science, 2018, 361, 278-281

378	Data inversion methods to determine sub-3 nm aerosol size distributions using the particle size magnifier. 2018 , 11, 4477-4491	14
377	Gas phase transformation from organic acid to organic sulfuric anhydride: Possibility and atmospheric fate in the initial new particle formation. 2018 , 212, 504-512	21
376	Concentration and size distribution of water-extracted dimethylaminium and trimethylaminium in atmospheric particles during nine campaigns - Implications for sources, phase states and formation pathways. 2018 , 631-632, 130-141	14
375	Rapid growth of organic aerosol nanoparticles over a wide tropospheric temperature range. 2018 , 115, 9122-9127	73
374	Uptake of water by an acid-base nanoparticle: theoretical and experimental studies of the methanesulfonic acid-methylamine system. 2018 , 20, 22249-22259	12
373	New particle formation leads to cloud dimming. 2018, 1,	12
372	Exploring atmospheric free-radical chemistry in China: the self-cleansing capacity and the formation of secondary air pollution. 2019 , 6, 579-594	57
371	Review of sub-3 nm condensation particle counters, calibrations, and cluster generation methods. 2019 , 53, 1277-1310	17
370	Global Modeling of Secondary Organic Aerosol With Organic Nucleation. 2019 , 124, 8260-8286	10
369	The heterogeneous reaction of dimethylamine/ammonia with sulfuric acid to promote the growth of atmospheric nanoparticles. 2019 , 6, 2767-2776	6
368	Remote Sensing Observation of New Particle Formation Events with a (UV, VIS) Polarization Lidar. 2019 , 11, 1761	6
367	Temperature effects on sulfuric acid aerosol nucleation and growth: initial results from the TANGENT study. 2019 , 19, 8915-8929	11
366	Evolution of aqSOA from the Air-Liquid Interfacial Photochemistry of Glyoxal and Hydroxyl Radicals. 2019 , 53, 10236-10245	19
365	Effect of temperature on the formation of highly oxygenated organic molecules (HOMs) from alpha-pinene ozonolysis. 2019 , 19, 7609-7625	24
364	New Particle Formation in the Atmosphere: From Molecular Clusters to Global Climate. 2019 , 124, 7098-7146	95
363	A large source of cloud condensation nuclei from new particle formation in the tropics. 2019 , 574, 399-403	75
362	New Particle Formation: A Review of Ground-Based Observations at Mountain Research Stations. 2019 , 10, 493	14
361	New particle formation, growth and apparent shrinkage at a rural background site in western Saudi Arabia. 2019 , 19, 10537-10555	11

360	Optical and Physical Characteristics of the Lowest Aerosol Layers over the Yellow River Basin. 2019 , 10, 638	4
359	Nanocluster Aerosol Emissions of a 3D Printer. 2019 , 53, 13618-13628	13
358	Over a 10-year record of aerosol optical properties at SMEAR II. 2019 , 19, 11363-11382	13
357	Infrared Spectroscopy of Hydrogen-Bonding Interactions in Neutral Dimethylamine-Methanol Complexes. 2019 , 123, 10109-10115	9
356	An Atmospheric Cluster Database Consisting of Sulfuric Acid, Bases, Organics, and Water. 2019 , 4, 10965-109	74 ₃ 2
355	Role of base strength, cluster structure and charge in sulfuric-acid-driven particle formation. 2019 , 19, 9753-9768	29
354	Traffic-originated nanocluster emission exceeds H<sub>-driven photochemical new particle formation in an urban area. 2019 ,	
353	Simulation of the Optical and Thermal Properties of Multiple CoreBhell Atmospheric Fractal Soot Agglomerates under Visible Solar Radiation. 2019 , 123, 24225-24233	
352	Electrospray Ionization-Based Synthesis and Validation of Amine-Sulfuric Acid Clusters of Relevance to Atmospheric New Particle Formation. 2019 , 30, 2267-2277	8
351	Molecular Composition and Volatility of Nucleated Particles from ⊕inene Oxidation between -50 °C and +25 °C. 2019 , 53, 12357-12365	14
350	Overview of Sources and Characteristics of Nanoparticles in Urban Traffic-Influenced Areas. 2019 , 72, 15-28	36
349	100 Years of Progress in Cloud Physics, Aerosols, and Aerosol Chemistry Research. 2019 , 59, 11.1-11.72	16
348	Molecular identification of organic vapors driving atmospheric nanoparticle growth. 2019, 10, 4442	37
347	Temperature Effects on Sulfuric Acid Aerosol Nucleation and Growth: Initial Results from the TANGENT Study. 2019 ,	
346	Decrease in radiative forcing by organic aerosol nucleation, climate, and land use change. 2019 , 10, 423	27
345	Growth of Aitken mode ammonium sulfate particles by Epinene ozonolysis. 2019 , 53, 406-418	7
344	Monte Carlo simulations of homogeneous nucleation and particle growth in the presence of background particles. 2019 , 71, 1554415	4
343	Particle Formation in a Complex Environment. 2019 , 10, 275	5

342	Multiphase chemistry in the troposphere: It all starts and ends with gases. 2019, 51, 736-752	4
341	Analysis of new particle formation (NPF) events at nearby rural, urban background and urban roadside sites. 2019 , 19, 5679-5694	20
340	Dynamic and timing properties of new aerosol particle formation and consecutive growth events. 2019 , 19, 5835-5852	10
339	Inversely modeling homogeneous H ₂ SO ₄ IH ₂ O nucleation rate in exhaust-related conditions. 2019 , 19, 6367-6388	5
338	Vertical profiles of sub-3 nm particles over the boreal forest. 2019 , 19, 4127-4138	13
337	Characteristics and mixing state of aerosol at the summit of Mount Tai (1534 m) in Central East China: First measurements with SPAMS. 2019 , 213, 273-284	12
336	Enhancement of Atmospheric Nucleation by Highly Oxygenated Organic Molecules: A Density Functional Theory Study. 2019 , 123, 5367-5377	5
335	Theoretical study of the cis-pinonic acid and its atmospheric hydrolysate participation in the atmospheric nucleation. 2019 , 674, 234-241	8
334	Unexpected Growth Coordinate in Large Clusters Consisting of Sulfuric Acid and CHO Tricarboxylic Acid. 2019 , 123, 3170-3175	11
333	Voltammetric Determination of the Stochastic Formation Rate and Geometry of Individual H N, and O Bubble Nuclei. 2019 , 13, 6330-6340	29
332	Molecular-Level Understanding of Synergistic Effects in Sulfuric Acid-Amine-Ammonia Mixed Clusters. 2019 , 123, 2420-2425	38
331	Improving new particle formation simulation by coupling a volatility-basis set (VBS) organic aerosol module in NAQPMS+APM. 2019 , 204, 1-11	18
330	Interannual and Seasonal Dynamics of Volatile Organic Compound Fluxes From the Boreal Forest Floor. 2019 , 10, 191	18
329	Problems Caused by Moisture in Gas Chromatographic Analysis of Headspace SPME Samples of Short-Chain Amines. 2019 , 82, 307-316	5
328	Atmospheric new particle formation in China. 2019 , 19, 115-138	73
327	Ion Mobility-Mass Spectrometry of Iodine Pentoxide-Iodic Acid Hybrid Cluster Anions in Dry and Humidified Atmospheres. 2019 , 10, 1935-1941	16
326	Sulfuric acid and aromatic carboxylate clusters H2SO4[ArCOOE]Structures, properties, and their relevance to the initial aerosol nucleation. 2019 , 439, 27-33	5
325	Observation of atmospheric new particle growth events at the summit of mountain Tai (1534 m) in Central East China. 2019 , 201, 148-157	12

324	Highly Oxygenated Organic Molecules (HOM) from Gas-Phase Autoxidation Involving Peroxy Radicals: A Key Contributor to Atmospheric Aerosol. 2019 , 119, 3472-3509	262
323	A proxy for atmospheric daytime gaseous sulfuric acid concentration in urban Beijing. 2019 , 19, 1971-1983	26
322	Understanding Hygroscopic Nucleation of Sulfate Aerosols: Combination of Molecular Dynamics Simulation with Classical Nucleation Theory. 2019 , 10, 1126-1132	3
321	Desert dust episodes over the Region of Balkan Peninsula. 2019 ,	
320	Urban Aerosol Particle Size Characterization in Eastern Mediterranean Conditions. 2019, 10, 710	9
319	Impact of a hydrophobic ion on the early stage of atmospheric aerosol formation. 2019 , 116, 22540-22544	4
318	Fission of charged nano-hydrated ammonia clusters - microscopic insights into the nucleation processes. 2019 , 21, 25749-25762	4
317	New particle formation in the volcanic eruption plume of the Piton de la Fournaise: specific features from a long-term dataset. 2019 , 19, 13243-13265	5
316	The influence of wind speed on new particle formation events in an urban environment. 2019 , 215, 37-41	11
315	A density functional theory study of the molecular interactions between a series of amides and sulfuric acid. 2019 , 214, 781-790	15
314	Intramolecular Hydrogen Shift Chemistry of Hydroperoxy-Substituted Peroxy Radicals. 2019 , 123, 590-600	22
313	Chemical Characterization of Highly Functionalized Organonitrates Contributing to Night-Time Organic Aerosol Mass Loadings and Particle Growth. 2019 , 53, 1165-1174	36
312	Chemical transformations in monoterpene-derived organic aerosol enhanced by inorganic composition. 2019 , 2,	25
311	Atmospheric Reactive Nitrogen in China. 2020 ,	1
310	What caused severe air pollution episode of November 2016 in New Delhi?. 2020, 222, 117125	53
309	Atmospheric implications of hydration on the formation of methanesulfonic acid and methylamine clusters: A theoretical study. 2020 , 244, 125538	12
308	Role of glycine on sulfuric acid-ammonia clusters formation: Transporter or participator. 2020 , 89, 125-135	4
307	Atmospheric Sulfuric Acid-Dimethylamine Nucleation Enhanced by Trifluoroacetic Acid. 2020 , 47, e2019GL08	5627

306	Formation mechanism of methanesulfonic acid and ammonia clusters: A kinetics simulation study. 2020 , 222, 117161	14
305	Characteristics and potential source areas of aliphatic amines in PM2.5 in Yangzhou, China. 2020 , 11, 296-302	11
304	Effects of forests on particle number concentrations in near-road environments across three geographic regions. 2020 , 266, 115294	7
303	The potential role of organics in new particle formation and initial growth in the remote tropical upper troposphere. 2020 ,	
302	Particle formation and surface processes on atmospheric aerosols: A review of applied quantum chemical calculations. 2020 , 120, e26350	10
301	Determinant Factor for Thermodynamic Stability of Sulfuric Acid-Amine Complexes. 2020 , 124, 10246-10257	2
300	Structures, energetics, and infrared spectra of the cationic monomethylamine-water clusters 2020 , 33, 31-36	1
299	Unprecedented Ambient Sulfur Trioxide (SO) Detection: Possible Formation Mechanism and Atmospheric Implications. 2020 , 7, 809-818	14
298	Deepening into the nucleation and fission processes of nano-hydrated ammonia clusters - a combined theoretical and experimental study. 2020 , 1412, 202030	
297	Establishing the structural motifs present in small ammonium and aminium bisulfate clusters of relevance to atmospheric new particle formation. 2020 , 153, 034307	7
296	Application of purge and trap-atmospheric pressure chemical ionization-tandem mass spectrometry for the determination of dimethyl sulfide in seawater. 2020 , 18, 547-559	3
295	. 2020,	3
294	Comparison of MODIS- and CALIPSO-Derived Temporal Aerosol Optical Depth over Yellow River Basin (China) from 2007 to 2015. 2020 , 4, 535-550	9
293	Molecular Specificity and Proton Transfer Mechanisms in Aerosol Prenucleation Clusters Relevant to New Particle Formation. 2020 , 53, 2816-2827	6
292	Frequent new particle formation over the high Arctic pack ice by enhanced iodine emissions. 2020 , 11, 4924	35
291	Catalytic activity of water molecules in gas-phase glycine dimerization. 2020 , 120, e26469	2
290	Atmospherically Relevant Hydrogen-Bonded Interactions between Methanesulfonic Acid and HSO Clusters: A Computational Study. 2020 , 124, 11072-11085	4
289	Spatio-Temporal Characteristics of PM2.5, PM10, and AOD over Canal Head Taocha Station, Henan Province. 2020 , 12, 3432	1

(2020-2020)

288	Sodium and lithium ions in aerosol: thermodynamic and rayleigh light scattering properties. 2020 , 139, 1	1
287	Interactions of sulfuric acid with common atmospheric bases and organic acids: Thermodynamics and implications to new particle formation. 2020 , 95, 130-140	6
286	Indoor Particulate Matter during HOMEChem: Concentrations, Size Distributions, and Exposures. 2020 , 54, 7107-7116	64
285	Rapid growth of new atmospheric particles by nitric acid and ammonia condensation. 2020 , 581, 184-189	72
284	Volatile organic compounds enhancing sulfuric acid-based ternary homogeneous nucleation: The important role of synergistic effect. 2020 , 233, 117609	2
283	Atmospheric New Particle Formation and Cloud Condensation Nuclei. 2020 , 415-451	
282	Field Observations of Secondary Organic Aerosols. 2020 , 453-508	
281	A molecular-scale study on the role of methanesulfinic acid in marine new particle formation. 2020 , 227, 117378	7
280	Hydration of Atmospheric Molecular Clusters III: Procedure for Efficient Free Energy Surface Exploration of Large Hydrated Clusters. 2020 , 124, 5253-5261	10
279	Size-dependent influence of NO on the growth rates of organic aerosol particles. 2020 , 6, eaay4945	28
278	Assessment of the DLPNO Binding Energies of Strongly Noncovalent Bonded Atmospheric Molecular Clusters. 2020 , 5, 7601-7612	24
277	Comparative analysis of local and global atmospheric electric field at the Northern Pakistan. 2020 , 206, 105326	2
276	Optical and Physical Characteristics of Aerosol Vertical Layers over Northeastern China. 2020 , 11, 501	7
275	Formation of highly oxygenated organic molecules from chlorine-atom-initiated oxidation of alpha-pinene. 2020 , 20, 5145-5155	10
274	Atmospheric chemistry of thiourea: nucleation with urea and roles in NO hydrolysis. 2020 , 22, 8109-8117	4
273	New mechanistic pathways for the formation of organosulfates catalyzed by ammonia and carbinolamine formation catalyzed by sulfuric acid in the atmosphere. 2020 , 22, 8800-8807	16
272	A possible unaccounted source of atmospheric sulfate formation: amine-promoted hydrolysis and non-radical oxidation of sulfur dioxide. 2020 , 11, 2093-2102	3
271	Ten-year global particulate mass concentration derived from space-borne CALIPSO lidar observations. 2020 , 721, 137699	18

270	Determination of the amine-catalyzed SO hydrolysis mechanism in the gas phase and at the air-water interface. 2020 , 252, 126292	4
269	Insights into atmospheric oxidation processes by performing factor analyses on subranges of mass spectra. 2020 , 20, 5945-5961	6
268	Atmospheric aerosol properties at a semi-rural location in southern India: particle size distributions and implications for cloud droplet formation. 2020 , 2, 1	7
267	Enhanced growth rate of atmospheric particles from sulfuric acid. 2020 , 20, 7359-7372	21
266	Modeling the formation and growth of atmospheric molecular clusters: A review. 2020 , 149, 105621	40
265	Variation of size-segregated particle number concentrations in wintertime Beijing. 2020 , 20, 1201-1216	32
264	Biogenic volatile organic compounds (BVOCs) reactivity related to new particle formation (NPF) over the Landes forest. 2020 , 237, 104869	11
263	Formation and growth of sub-3-nm aerosol particles in experimental chambers. 2020 , 15, 1013-1040	21
262	Traffic-originated nanocluster emission exceeds H<sub>-driven photochemical new particle formation in an urban area. 2020 , 20, 1-13	22
261	Ultrafine Particle Number Concentration Model for Estimating Retrospective and Prospective Long-Term Ambient Exposures in Urban Neighborhoods. 2020 , 54, 1677-1686	9
260	Atmospheric fungal nanoparticle bursts. 2020 , 6, eaax9051	12
259	Atmospheric implication of synergy in methanesulfonic acid-base trimers: a theoretical investigation 2020 , 10, 5173-5182	11
258	On the regional aspects of new particle formation in the Eastern Mediterranean: A comparative study between a background and an urban site based on long term observations. 2020 , 239, 104911	7
257	2-Methyltetrol sulfate ester-initiated nucleation mechanism enhanced by common nucleation precursors: A theory study. 2020 , 723, 137987	3
256	Aerosol Optical Properties and Contribution to Differentiate Haze and Haze-Free Weather in Wuhan City. 2020 , 11, 322	3
255	On the fate of oxygenated organic molecules in atmospheric aerosol particles. 2020 , 6, eaax8922	31
254	The impact of the atmospheric turbulence-development tendency on new particle formation: a common finding on three continents. 2021 , 8, nwaa157	4
253	Characterization of raindrop size distributions and its response to cloud microphysical properties. 2021 , 249, 105292	6

(2021-2021)

252	Formation and growth of sub-3[hm particles in megacities: impact of background aerosols. 2021 , 226, 348-363	13
251	The size-mobility relationship of ions, aerosols, and other charged particle matter 2021 , 151, 105659	12
250	A theoretical study of hydrogen-bonded molecular clusters of sulfuric acid and organic acids with amides. 2021 , 100, 328-339	4
249	Secondary aerosol formation in winter haze over the Beijing-Tianjin-Hebei Region, China. 2021 , 15, 1	21
248	Research agenda for the Russian Far East and utilization of multi-platform comprehensive environmental observations. 2021 , 14, 311-337	6
247	Study of new particle formation events in southern Italy. 2021 , 244, 117920	7
246	The formation mechanism and radiative effect of secondary organic aerosols. 2021, 57-100	
245	Hydration motifs of ammonium bisulfate clusters show complex temperature dependence. 2021 , 154, 014304	4
244	Long-term measurement of sub-3 nm particles and their precursor gases in the boreal forest. 2021 , 21, 695-715	7
243	Molecular properties affecting the hydration of acid-base clusters. 2021 , 23, 13106-13114	2
242	New particle formation from agricultural recycling of organic waste products. 2021, 4,	1
241	Surface active agents stabilize nanodroplets and enhance haze formation. 2021 , 30, 010504	
240	Role of iodine oxoacids in atmospheric aerosol nucleation. <i>Science</i> , 2021 , 371, 589-595	31
239	Influence of vegetation on occurrence and time distributions of regional new aerosol particle formation and growth. 2021 , 21, 2861-2880	2
238	Radiatively driven NH3 release from agricultural field during wintertime slack season. 2021 , 247, 118228	1
237	Large Discrepancy in the Formation of Secondary Organic Aerosols from Structurally Similar Monoterpenes. 2021 , 5, 632-644	3
236	Clusteromics I: Principles, Protocols, and Applications to Sulfuric Acid-Base Cluster Formation. 2021 , 6, 7804-7814	9
235	The seasonal cycle of ice-nucleating particles linked to the abundance of biogenic aerosol in boreal forests. 2021 , 21, 3899-3918	11

234	New Particle Formation and Growth from Dimethyl Sulfide Oxidation by Hydroxyl Radicals. 2021 , 5, 801-811	4
233	Impact of Urban Pollution on Organic-Mediated New-Particle Formation and Particle Number Concentration in the Amazon Rainforest. 2021 , 55, 4357-4367	2
232	The Synergistic Role of Sulfuric Acid, Bases, and Oxidized Organics Governing New-Particle Formation in Beijing. 2021 , 48, e2020GL091944	23
231	New Particle Formation and Growth to Climate-Relevant Aerosols at a Background Remote Site in the Western Himalaya. 2021 , 126, e2020JD033267	6
230	Road traffic nanoparticle characteristics: Sustainable environment and mobility. 2021, 13, 101196	7
229	More Significant Impacts From New Particle Formation on Haze Formation During COVID-19 Lockdown. 2021 , 48, e2020GL091591	8
228	Influence of atmospheric conditions on the role of trifluoroacetic acid in atmospheric sulfuric aciddimethylamine nucleation. 2021 , 21, 6221-6230	5
227	Formation of nighttime sulfuric acid from the ozonolysis of alkenes in Beijing. 2021 , 21, 5499-5511	5
226	Past, present, and future of ultrafine particle exposures in North America. 2021 , 10, 100109	3
225	Enhancement of nanoparticle formation and growth during the COVID-19 lockdown period in urban Beijing. 2021 , 21, 7039-7052	3
224	Molecular characterization of gaseous and particulate oxygenated compounds at a remote site in Cape Corsica in the western Mediterranean Basin. 2021 , 21, 8067-8088	3
223	Sesquiterpenes and oxygenated sesquiterpenes dominate the VOC (C₅¶₂₀) emissions of downy birches. 2021 , 21, 8045-8066	1
222	Molecular-Scale Mechanism of Sequential Reaction of Oxalic Acid with SO: Potential Participator in Atmospheric Aerosol Nucleation. 2021 , 125, 4200-4208	2
221	Measurement report: Molecular composition and volatility of gaseous organic compounds in a boreal forest I from volatile organic compounds to highly oxygenated organic molecules. 2021 , 21, 8961-8977	1
220	Urban aerosol size distributions: a global perspective. 2021 , 21, 8883-8914	8
219	Towards understanding the characteristics of new particle formation in the Eastern Mediterranean. 2021 , 21, 9223-9251	4
218	Large hemispheric difference in nucleation mode aerosol concentrations in the lowermost stratosphere at mid- and high latitudes. 2021 , 21, 9065-9088	1
217	GlobalEegional nested simulation of particle number concentration by combing microphysical processes with an evolving organic aerosol module. 2021 , 21, 9343-9366	5

216	Discovery of a Potent Source of Gaseous Amines in Urban China. 2021, 8, 725-731	6
215	Valine involved sulfuric acid-dimethylamine ternary homogeneous nucleation and its atmospheric implications. 2021 , 254, 118373	2
214	New particle formation and its CCN enhancement in the Yangtze River Delta under the control of continental and marine air masses. 2021 , 254, 118400	
213	Atmospheric and ecosystem big data providing key contributions in reaching United Nations Sustainable Development Goals. 2021 , 5, 277-305	2
212	Contribution of New Particle Formation to Cloud Condensation Nuclei Activity and its Controlling Factors in a Mountain Region of Inland China. 2021 , 126, e2020JD034302	0
211	Impact of aerosolEadiation interaction on new particle formation. 2021 , 21, 9995-10004	3
210	Wide-field optical sizing of single nanoparticles with 10 nm accuracy. 2021 , 64, 1	
209	Observational Evidence of Lightning-Generated Ultrafine Aerosols. 2021 , 48, e2021GL093771	6
208	Observation of sub-3nm particles and new particle formation at an urban location in India. 2021 , 256, 118460	3
207	Characterization of aerosol number size distributions and their effect on cloud properties at Syowa Station, Antarctica. 2021 , 21, 12155-12172	2
206	Zeppelin-led study on the onset of new particle formation in the planetary boundary layer. 2021 , 21, 12649-12663	5
205	In situ observation of new particle formation (NPF) in the tropical tropopause layer of the 2017 Asian monsoon anticyclone Part 1: Summary of StratoClim results. 2021 , 21, 11689-11722	4
204	Analysis of Positive and Negative Atmospheric Air Ions During New Particle Formation (NPF) Events over Urban City of India. 1	2
203	Theoretical study of the formation and nucleation mechanism of highly oxygenated multi-functional organic compounds produced by pinene. 2021 , 780, 146422	2
202	A phenomenology of new particle formation (NPF) at 13 European sites. 2021 , 21, 11905-11925	4
201	Spatial variations in urban air pollution: impacts of diesel bus traffic and restaurant cooking at small scales. 1	1
200	Air Pollution, Health and Perception.	
199	Tri-Base Synergy in Sulfuric Acid-Base Clusters. 2021 , 12, 1260	3

198	Characterization of submicron aerosols over the Yellow Sea measured onboard the Gisang 1 research vessel in the spring of 2018 and 2019. 2021 , 284, 117180	2
197	Investigation of Particle Number Concentrations and New Particle Formation With Largely Reduced Air Pollutant Emissions at a Coastal Semi-Urban Site in Northern China. 2021 , 126, e2021JD035419	2
196	Interactions between isocyanic acid and atmospheric acidic, neutral and basic species. 2021, 1204, 113384	1
195	Organic acid-ammonia ion-induced nucleation pathways unveiled by quantum chemical calculation and kinetics modeling: A case study of 3-methyl-1,2,3-butanetricarboxylic acid. 2021 , 284, 131354	O
194	Aerosols in Atmospheric Chemistry. 2022,	
193	Towards a concentration closure of sub-6 nm aerosol particles and sub-3 nm atmospheric clusters. 2022 , 159, 105878	1
192	Combining instrument inversions for sub-10 nm aerosol number size-distribution measurements. 2022 , 159, 105862	1
191	Direct measurement of curvature-dependent surface tension of an alcohol nanomeniscus. 2021 , 13, 6991-69	961
190	Emerging Investigator Series: COVID-19 lockdown effects on aerosol particle size distributions in northern Italy. 2021 , 1, 214-227	3
189	Propionamide participating in HSO-based new particle formation: a theory study 2020 , 11, 493-500	3
188	Recent advances in understanding secondary organic aerosol: Implications for global climate forcing. 2017 , 55, 509-559	359
187	Sources and formation of nucleation mode particles in remote tropical marine atmospheres over the South China Sea and the Northwest Pacific Ocean. 2020 , 735, 139302	6
186	Characteristics of Aerosol and Cloud Condensation Nuclei Concentrations Measured over the Yellow Sea on a Meteorological Research Vessel, GISANG 1. 2016 , 26, 243-256	2
185	Harnessing remote sensing to address critical science questions on ocean-atmosphere interactions. 2018 , 6,	11
184	Data_Sheet_1.CSV. 2019 ,	0
183	Sources and sinks driving sulfuric acid concentrations in contrasting environments: implications on proxy calculations. 2020 , 20, 11747-11766	20
182	Decennial time trends and diurnal patterns of particle number concentrations in a central European city between 2008 and 2018. 2020 , 20, 12247-12263	7
181	The Aarhus Chamber Campaign on Highly Oxygenated Organic Molecules and Aerosols (ACCHA): particle formation, organic acids, and dimer esters from <i></i>-pinene ozonolysis at different temperatures. 2020 , 20, 12549-12567	6

180	New particle formation at urban and high-altitude remote sites in the south-eastern Iberian Peninsula. 2020 , 20, 14253-14271	12
179	The potential role of organics in new particle formation and initial growth in the remote tropical upper troposphere. 2020 , 20, 15037-15060	4
178	Molecular understanding of new-particle formation from <i></i>-pinene between B 0 and +25 LC. 2020 , 20, 9183-9207	32
177	Identification and quantification of particle growth channels during new particle formation.	1
176	Enhancement of atmospheric H ₂ SO ₄ /H ₂ O nucleation: organic oxidation products versus amines.	6
175	The direct and indirect radiative effects of biogenic secondary organic aerosol.	6
174	Aerosols and nucleation in Eastern China: first insights from the new SORPES-Station.	1
173	Total sulphate vs. sulphuric acid monomer in nucleation studies: which represents the "true" concentration?.	2
172	Analysis of feedbacks between nucleation rate, survival probability and cloud condensation nuclei formation.	1
171	Technical Note: Using DEG CPCs at upper tropospheric temperatures.	1
170	Electrical charging changes the composition of sulfuric acid-ammonia/dimethylamine clusters.	2
169	Submicron aerosols at thirteen diversified sites in China: size distribution, new particle formation and corresponding contribution to cloud condensation nuclei production.	2
168	Ion particle interactions during particle formation and growth at a coniferous forest site in central Europe.	1
167	Forest canopy interactions with nucleation mode particles.	2
166	Impacts of new particle formation on aerosol cloud condensation nuclei (CCN) activity in Shanghai: case study.	2
165	Strong atmospheric new particle formation in winter, urban Shanghai, China.	2
164	lodine observed in new particle formation events in the Arctic atmosphere during ACCACIA.	1
163	Reactivity of stabilized Criegee intermediates (sCI) from isoprene and monoterpene ozonolysis toward SO ₂ and organic acids.	7

162	A chamber study of the influence of boreal BVOC emissions and sulphuric acid on nanoparticle formation rates at ambient concentrations.	3
161	Modeling ultrafine particle growth at a pine forest site influenced by anthropogenic pollution during BEACHON-RoMBAS 2011.	3
160	Analysis of nucleation events in the European boundary layer using the regional aerosol-climate model REMO-HAM with a solar radiation-driven OH-proxy.	1
159	Variability of air ion concentrations in urban Paris.	1
158	Biotic stress accelerates formation of climate-relevant aerosols in boreal forests.	4
157	Aerosol size distribution and new particle formation in western Yangtze River Delta of China: two-year measurement at the SORPES station.	3
156	Thermodynamics of the formation of sulfuric acid dimers in the binary (H ₂ 5O ₄ -H ₂ 0) and ternary (H ₂ O-NH ₃ 4420-NH ₃ 44420-NH ₃ 44<	ıgt;)
155	system. Nucleation and growth of sub-3 nm particles in the polluted urban atmosphere of a megacity in China.	3
154	Formation of highly oxidized multifunctional compounds: autoxidation of peroxy radicals formed in the ozonolysis of alkenes Ideduced from structure product relationships.	6
153	Observation of viscosity transition in pinene secondary organic aerosol.	4
152	Synergistic use of Lagrangian dispersion modelling, satellite and surface remote sensing measurements for the investigation of volcanic plumes: the Mount Etna eruption of 2507 October 2013.	2
151	Experimental investigation of ion-ion recombination at atmospheric conditions.	2
150	Size-resolved cloud condensation nuclei concentration measurements in the Arctic: two case studies from the summer of 2008.	2
149	Particulate matter, air quality and climate: lessons learned and future needs.	12
148	Contribution from biogenic organic compounds to particle growth during the 2010 BEACHON-ROCS campaign in a Colorado temperate needle leaf forest.	2
147	A new high transmission inlet for the Caltech nano-RDMA for size distribution measurements of sub-3 nm ions at ambient concentrations.	1
146	Trimethylamine emissions in animal husbandry.	1
145	Modelling the dispersion of particle numbers in five European cities.	O

144	Characterizing Atmospheric Aerosols off the Atlantic Canadian Coast During C-FOG. 2021 , 181, 345	
143	Formation of condensable organic vapors from anthropogenic and biogenic volatile organic compounds (VOCs) is strongly perturbed by NO_{<i>x</i>} in eastern China. 2021 , 21, 14789-14814	3
142	Ozone Initiates Human-Derived Emission of Nanocluster Aerosols. 2021 , 55, 14536-14545	3
141	Vibrational Spectra of Atmospherically Relevant Hydrogen-Bonded MSA∭(HSO) (= 1-3) Clusters. 2021 , 125, 8791-8802	
140	Reduced volatility of aerosols from surface emissions to the top of the planetary boundary layer. 2021 , 21, 14749-14760	2
139	Semi-empirical parameterization of size-dependent atmospheric nanoparticle growth in continental environments.	1
138	Estimating neutral nanoparticle steady state size distribution and growth according to measurements of intermediate air ions.	
137	Estimating the contribution of ionIbn recombination to sub-2 nm cluster concentrations from atmospheric measurements.	
136	Growth of sulphuric acid nanoparticles under wet and dry conditions.	
135	Suppression of new particle formation from monoterpene oxidation by NO _x .	
134	New foliage growth is a significant, unaccounted source for volatiles in boreal evergreen forests.	
133	Comparing three vegetation monoterpene emission models to measured gas concentrations with a model of meteorology, air chemistry and chemical transport.	
133		1
	model of meteorology, air chemistry and chemical transport.	1
132	model of meteorology, air chemistry and chemical transport. Chemistry of new particle growth in mixed urban and biogenic emissions linsights from CARES.	1
132	model of meteorology, air chemistry and chemical transport. Chemistry of new particle growth in mixed urban and biogenic emissions linsights from CARES. Production and growth of new particles during two cruise campaigns in the marginal seas of China.	1
132 131 130	model of meteorology, air chemistry and chemical transport. Chemistry of new particle growth in mixed urban and biogenic emissions [Insights from CARES. Production and growth of new particles during two cruise campaigns in the marginal seas of China. Introduction. 2014, 1-34	1

126	On the composition of ammonia-sulfuric acid clusters during aerosol particle formation.	Ο
125	Major contribution of neutral clusters to new particle formation in the free troposphere.	1
124	On the derivation of particle nucleation rates from experimental formation rates.	
123	Total sulphate vs. sulphuric acid monomer in nucleation studies.	
122	Investigation into chemistry of new particle formation and growth in subtropical urban environment.	
121	Scanning supersaturation CPC applied as a nano-CCN counter for size-resolved analysis of the hygroscopicity and chemical composition of nanoparticles.	
120	Elemental composition and clustering of pinene oxidation products for different oxidation conditions.	
119	Technical Note: New particle formation event forecasts during PEGASOS-Zeppelin Northern mission 2013 in Hyytil Finland.	
118	Impact of gas-to-particle partitioning approaches on the simulated radiative effects of biogenic secondary organic aerosol.	
117	Ideas and Perspectives: On the emission of amines from terrestrial vegetation in the context of atmospheric new particle formation.	
116	Airborne measurements of new particle formation in the free troposphere above the Mediterranean Sea during the HYMEX campaign.	0
115	Relating the hygroscopic properties of submicron aerosol to both gas- and particle-phase chemical composition in a boreal forest environment.	
114	Seasonality of ultrafine and sub-micron aerosols and the inferences on particle formation processes.	
113	Introduction: The Pan-Eurasian Experiment (PEEX) Imulti-disciplinary, multi-scale and multi-component research and capacity building initiative.	
112	Molecular corridors and parameterizations of volatility in the evolution of organic aerosols.	
111	High concentrations of sub-3 nm clusters and frequent new particle formation observed in the Po Valley, Italy, during the PEGASOS 2012 campaign.	
110	Technical note: Detection of dimethylamine in the low pptv range using nitrate Chemical Ionization-Atmospheric Pressure interface-Time Of Flight (CI-APi-TOF) mass spectrometry.	
109	Cosmic rays and aerosols in the terrestrial atmosphere. 2018 , 15-27	

108 Everyone Is Exposed Every Day. **2018**, 41-56

107	Contribution of Atmospheric Reactive Nitrogen to Haze Pollution in China. 2020 , 113-134	
106	The synergistic effects of methanesulfonic acid (MSA) and methane-sulfinic acid (MSIA) on marine new particle formation. 2021 , 269, 118826	О
105	Drought effects on volatile organic compound emissions from Scots pine stems. 2021,	1
104	A molecular dynamics study of collisional heat transfer to nanoclusters in the gas phase. 2022 , 159, 105891	2
103	Impact of sub-grid particle formation in sulfur-rich plumes on particle mass and number concentrations over China. 2022 , 268, 118711	
102	Comparison results of eight oxygenated organic molecules: Unexpected contribution to new particle formation in the atmosphere. 2022 , 268, 118817	1
101	The standard operating procedure for Airmodus Particle Size Magnifier and nano-Condensation Nucleus Counter. 2022 , 159, 105896	1
100	Long-term trend of new particle formation events in the Yangtze River Delta, China and its influencing factors: 7-year dataset analysis. 2021 , 807, 150783	1
99	Observations of Gas-Phase Alkylamines at a Coastal Site in the East Mediterranean Atmosphere. 2021 , 12, 1454	1
98	Modelling the influence of biotic plant stress on atmospheric aerosol particle processes throughout a growing season. 2021 , 21, 17389-17431	1
97	Wintertime subarctic new particle formation from Kola Peninsula sulfur emissions. 2021 , 21, 17559-17576	2
96	Variations in Source Contributions of Particle Number Concentration Under Long-Term Emission Control in Winter of Urban Beijing.	
95	Reduction in Anthropogenic Emissions Suppressed New Particle Formation and Growth: Insights From the COVID-19 Lockdown. 2022 , 127, e2021JD035392	O
94	Analysis and research of absorbing aerosols in Beijing-Tianjin-Hebei region. 1	О
93	Study on Vertically Distributed Aerosol Optical Characteristics over Saudi Arabia Using CALIPSO Satellite Data. 2022 , 12, 603	
92	Protonated acetone ion chemical ionization time-of-flight mass spectrometry for real-time measurement of atmospheric ammonia 2022 , 114, 66-74	О
91	Effects of oligomerization and decomposition on the nanoparticle growth: a model study. 2022 , 22, 155-171	

90	Quantum Machine Learning Approach for Studying Atmospheric Cluster Formation.	5
89	A theoretical perspective on the structure and thermodynamics of secondary organic aerosols from toluene: molecular hierarchical synergistic effects.	
88	The reaction of Criegee intermediates with formamide and its implication to atmospheric aerosols 2022 , 296, 133717	О
87	Classical and Nonclassical Nucleation and Growth Mechanisms for Nanoparticle Formation 2022,	2
86	Activation of sub-3 nm organic particles in the particle size magnifier using humid and dry conditions. 2022 , 161, 105945	О
85	The origin of enhanced $$\{\{\{\{\{\{m\{O\}\}\}\}\}\}\}\}$ 2 $^{+}$ \$ production from photoionized CO2 clusters. 2022 , 5,	O
84	First eddy covariance flux measurements of semi-volatile organic compounds with the PTR3-TOF-MS. 2021 , 14, 8019-8039	1
83	Tropical and Boreal Forest [Atmosphere Interactions: A Review. 2022 , 74, 24-163	1
82	Vacuum ultraviolet free-electron laser photoionization mass spectrometry of alpha-pinene ozonolysis.	
81	A theoretical study on the formation mechanism of carboxylic sulfuric anhydride and its potential role in new particle formation 2022 , 12, 5501-5508	1
80	Frequent new particle formation at remote sites in the subboreal forest of North America. 2022 , 22, 2487-2505	2
79	Measurement report: Long-term measurements of aerosol precursor concentrations in the Finnish subarctic boreal forest. 2022 , 22, 2237-2254	1
78	Hydrogen-Bond Topology Is More Important Than Acid/Base Strength in Atmospheric Prenucleation Clusters 2022 ,	4
77	Emission of volatile organic compounds by plants on the floor of boreal and mid-latitude forests. 1	O
76	Theoretical Investigation on the Oligomerization of Methylglyoxal and Glyoxal in Aqueous Atmospheric Aerosol Particles.	О
75	Particle Number Concentration: A Case Study for Air Quality Monitoring. 2022 , 13, 570	0
74	Variations in source contributions of particle number concentration under long-term emission control in winter of urban Beijing 2022 , 119072	2
73	Influence of biogenic emissions from boreal forests on aerosoldloud interactions. 2022 , 15, 42-47	1

72	Advancing the science of dynamic airborne nanosized particles using Nano-DIHM. 2021, 4,	0
71	What controls the observed size-dependency of the growth rates of sub-10 nm atmospheric particles?.	О
70	Estimation of nucleation barrier in multicomponent system with intermolecular potential.	
69	Measurement report: Introduction to the HyICE-2018 campaign for measurements of ice-nucleating particles and instrument inter-comparison in the Hyytillboreal forest. 2022 , 22, 5117-5145	O
68	Influence of Aerosol Chemical Composition on Condensation Sink Efficiency and New Particle Formation in Beijing 2022 , 9, 375-382	О
67	Microscopic Insights Into the Formation of Methanesulfonic AcidMethylamineAmmonia Particles Under Acid-Rich Conditions. 2022 , 10,	
66	Clusteromics III: Acid Synergy in Sulfuric Acid-Methanesulfonic Acid-Base Cluster Formation 2022 , 7, 15206-15214	3
65	Data_Sheet_2.CSV. 2019 ,	
64	Data_Sheet_3.CSV. 2019 ,	
63	Data_Sheet_4.pdf. 2019 ,	
63	Data_Sheet_4.pdf. 2019 , Iodous acid-a more efficient nucleation precursor than iodic acid.	1
		1
62	Iodous acid-a more efficient nucleation precursor than iodic acid. Determination of Gaseous and Particulate Secondary Amines in the Atmosphere Using Gas	1
62	Iodous acid-a more efficient nucleation precursor than iodic acid. Determination of Gaseous and Particulate Secondary Amines in the Atmosphere Using Gas Chromatography Coupled with Electron Capture Detection. 2022, 13, 664	1
62 61 60	Iodous acid-a more efficient nucleation precursor than iodic acid. Determination of Gaseous and Particulate Secondary Amines in the Atmosphere Using Gas Chromatography Coupled with Electron Capture Detection. 2022, 13, 664 Electrical Mobility as an Indicator for Flexibly Deducing the Kinetics of Nanoparticle Evaporation.	
62 61 60 59	lodous acid-a more efficient nucleation precursor than iodic acid. Determination of Gaseous and Particulate Secondary Amines in the Atmosphere Using Gas Chromatography Coupled with Electron Capture Detection. 2022, 13, 664 Electrical Mobility as an Indicator for Flexibly Deducing the Kinetics of Nanoparticle Evaporation. Molecular-level nucleation mechanism of iodic acid and methanesulfonic acid. 2022, 22, 6103-6114 Assessment of spatio-temporal trends of satellite-based aerosol optical depth using Mann&endall	2
62 61 60 59 58	lodous acid-a more efficient nucleation precursor than iodic acid. Determination of Gaseous and Particulate Secondary Amines in the Atmosphere Using Gas Chromatography Coupled with Electron Capture Detection. 2022, 13, 664 Electrical Mobility as an Indicator for Flexibly Deducing the Kinetics of Nanoparticle Evaporation. Molecular-level nucleation mechanism of iodic acid and methanesulfonic acid. 2022, 22, 6103-6114 Assessment of spatio-temporal trends of satellite-based aerosol optical depth using Mann&endall test and Sen® slope estimator model. 2022, 13, 1270-1298	2

54	Measurement report: Hygroscopic growth of ambient fine particles measured at five sites in China. 2022 , 22, 6773-6786	0
53	The proper view of cluster free energy in nucleation theories. 1-10	1
52	Institute for Atmospheric and Earth System Research (INAR): Showcases for making science diplomacy. 2022 , 58,	0
51	Role of gasholecular clusterBerosol dynamics in atmospheric new-particle formation. 2022 , 12,	1
50	Measurement report: Atmospheric new particle formation in a coastal agricultural site explained with binPMF analysis of nitrate CI-APi-TOF spectra. 2022 , 22, 8097-8115	0
49	Changes in the new particle formation and shrinkage events of the atmospheric ions during the COVID-19 lockdown. 2022 , 44, 101214	
48	Aerosol mass spectrometry of neutral species based on a tunable vacuum ultraviolet free electron laser. 2022 , 24, 16484-16492	0
47	Quiet New Particle Formation in the Atmosphere. 10,	1
46	Diurnal evolution of negative atmospheric ions above the boreal forest: from ground level to the free troposphere. 2022 , 22, 8547-8577	O
45	Investigation of new particle formation mechanisms and aerosol processes at Marambio Station, Antarctic Peninsula. 2022 , 22, 8417-8437	1
44	Nonisothermal nucleation in the gas phase is driven by cool subcritical clusters. 2022, 119,	O
43	Temporal variations, transport, and regional impacts of atmospheric aerosol and acid gases close to an oil and gas trading hub.	
42	Theoretical analysis of sulfuric aciddimethylaminebxalic aciddwater clusters and implications for atmospheric cluster formation. 2022 , 12, 22425-22434	
41	Computational chemistry of cluster: Understanding the mechanism of atmospheric new particle formation at the molecular level. 2022 , 136109	
40	Monoterpene Photooxidation in a Continuous-Flow Chamber: SOA Yields and Impacts of Oxidants, NOx, and VOC Precursors.	
39	Seasonal variation in oxygenated organic molecules in urban Beijing and their contribution to secondary organic aerosol. 2022 , 22, 10077-10097	O
38	Clusteromics IV: The Role of Nitric Acid in Atmospheric Cluster Formation.	1
37	Tutorial: Dynamic organic growth modeling with a volatility basis set. 2022 , 166, 106063	O

36	Molecular-level insight into uptake of dimethylamine on hydrated nitric acid clusters.	1
35	The Driving Effects of Common Atmospheric Molecules for Formation of Prenucleation Clusters: The Case of Sulfuric Acid, Formic Acid, Nitric Acid, Ammonia, and Dimethyl Amine.	2
34	Ultrafine Particle Emissions in the Mediterranean. 2022 , 105-123	3
33	Measurement report: A multi-year study on the impacts of Chinese New Year celebrations on air quality in Beijing, China. 2022 , 22, 11089-11104	O
32	The effectiveness of the coagulation sink of 3🛮 0 nm atmospheric particles. 2022, 22, 11529-11541	O
31	Peroxy Radical and Product Formation in the Gas-Phase Ozonolysis of Pinene under Near-Atmospheric Conditions: Occurrence of an Additional Series of Peroxy Radicals O,OII10H15O(O2)yO2 with y = 1IB. 2022, 126, 6526-6537	1
30	Turbulent Flux Measurements of the Near-Surface and Residual-Layer Small Particle Events. 2022 , 127,	0
29	Towards fully ab initio simulation of atmospheric aerosol nucleation. 2022 , 13,	O
28	On the relation between apparent ion and total particle growth rates in the boreal forest and related chamber experiments. 2022 , 22, 13153-13166	0
27	Reviews and syntheses: VOC emissions from soil cover in boreal and temperate natural ecosystems of the Northern Hemisphere. 2022 , 19, 4715-4746	O
26	Review of the influencing factors of secondary organic aerosol formation and aging mechanism based on photochemical smog chamber simulation methods. 2022 ,	1
25	Hygroscopicity and CCN potential of DMS-derived aerosol particles. 2022 , 22, 13449-13466	O
24	Geometricallydriven aggregation of anisotropic dielectric particles.	0
23	Vigorous New Particle Formation Above Polluted Boundary Layer in the North China Plain. 2022 , 49,	O
22	The critical role of dimethylamine in the rapid formation of iodic acid particles in marine areas. 2022 , 5,	1
21	Survival probability of new atmospheric particles: closure between theory and measurements from 1.4 to 100 nm. 2022 , 22, 14571-14587	O
20	Hygroscopicity of ultrafine particles containing ammonium/alkylaminium sulfates: A Käler model investigation with correction of surface tension. 2023 , 294, 119500	О
19	Measurement report: Increasing trend of atmospheric ion concentrations in the boreal forest. 2022 , 22, 15223-15242	O

18	Ocean Emission Pathway and Secondary Formation Mechanism of Aminiums Over the Chinese Marginal Sea. 2022 , 127,	0
17	Massive Assessment of the Binding Energies of Atmospheric Molecular Clusters. 2022 , 18, 7373-7383	O
16	On the influence of VOCs on new particle growth in a Continental-Mediterranean region.	O
15	Source characterization of volatile organic compounds in urban Beijing and its links to secondary organic aerosol formation. 2022 , 160469	O
14	Characters of Particulate Matter and Their Relationship with Meteorological Factors during Winter Nanyang 2021 2022. 2023, 14, 137	1
13	Bridging Gaps between Clusters in Molecular-Beam Experiments and Aerosol Nanoclusters. 2023 , 14, 287-294	O
12	Atmospheric Oxidation and Secondary Particle Formation. 2023, 19-91	Ο
11	An unexpectedly feasible route for the formation of organosulfates by the gas phase reaction of sulfuric acid with acetaldehyde catalyzed by dimethylamine in the atmosphere.	О
10	CO2 Aggregation on Monoethanolamine: Observation from Rotational Spectroscopy.	O
9	A new advance in pollution profile, transformation process, and contribution to SOA formation of atmospheric organic amines.	O
8	CO2 Aggregation on Monoethanolamine: Observation from Rotational Spectroscopy.	0
7	High frequency of new particle formation events driven by summer monsoon in the central Tibetan Plateau, China. 2023 , 23, 4343-4359	Ο
6	Reducing chemical complexity in representation of new-particle formation: evaluation of simplification approaches. 2023 , 3, 552-567	0
5	Advancing understanding of landਬtmosphere interactions by breaking discipline and scale barriers. 2023 , 1522, 74-97	O
4	High emission rates and strong temperature response make boreal wetlands a large source of isoprene and terpenes. 2023 , 23, 2683-2698	O
3	The neglected autoxidation pathways for the formation of highly oxygenated organic molecules (HOMs) and the nucleation of the HOMs generated by limonene. 2023 , 304, 119727	O
2	Analysis of new particle formation events and comparisons to simulations of particle number concentrations based on GEOS-ChemBdvanced particle microphysics in Beijing, China. 2023 , 23, 4091-4104	O
1	Size-dependent hygroscopicity of levoglucosan and D-glucose aerosol nanoparticles. 2023 , 23, 4763-4774	Ο